Avidin localizations in pH-responsive polymersomes for probing the docking of biotinylated (macro)molecules in the membrane and lumen

Silvia Moreno[a]*, Susanne Boye[a], Albena Lederer[a,b], Annarita Falanga[c], Stefania Galdiero[c], Sébastien Lecommandoux[d], Brigitte Voit[a,b], and Dietmar Appelhans[a]*

[a] Leibniz-Institut für Polymerforschung Dresden e.V., Hohe Straße 6, 01069 Dresden, Germany E-Mail: applhans@ipfdd.de; moreno@ipfdd.de

[b] Organic Chemistry of Polymers, Technische Universität Dresden, 01062 Dresden, Germany and Center for Advancing Electronics Dresden, 01062 Dresden, Germany

[c] Department of Pharmacy, University of Naples "Federico II", Via Mezzocannone 16, 80134 Naples, Italy; CiRPEB, University of Naples "Federico II", Via Mezzocannone 16, 80134 Naples, Italy

[d] Université de Bordeaux, ENSCPB, 16 avenue Pey Berland, 33607 Pessac Cedex, France; CNRS, Laboratoire de Chimie des Polymères Organiques, UMR5629, Pessac, France.

ABSTRACT: To mimic organelles and cells and to construct next generation therapeutics, asymmetric functionalization and location of proteins for artificial vesicles is thoroughly needed to emphasize the complex interplay of biological units and systems through spatially separated and spatiotemporal controlled actions, release and communications. For the challenge of vesicle (= polymersome) construction, the membrane permeability and the location of the cargo are important key characteristics that determine the potential applications of them. Herein, an *in situ* and *post* loading process of avidin in pH-responsive and photo-crosslinked polymersomes is developed and characterized. Firstly, loading efficiency, main location (inside, lumen, outside) and release of avidin under different conditions have been validated, including the pH-stable presence of avidin in polymersomes´ membrane outside and inside. This advantageous approach allows to selectively functionalize the outer and inner membrane as well the lumen with several bio(macro)molecules, generally suited for the construction of asymmetrically functionalized artificial organelles. In addition, a FRET effect was used to study the permeability or uptake of polymersomes membrane against a broad range of biotinylated (macro)molecules (different typology, sizes and shapes) at different conditions.

INTRODUCTION

The polymersomes, whose term originates from the structural analogy with liposomes, emerged as a versatile platform for creating biological and synthetic vesicles, such as nanoreactors, nanosensors, and containers with controlled uptake and release for the delivery of drugs and proteins and for imaging studies.[1-15] To understand deeply a system as complex as the cell is currently a great challenge for the scientific community. Therefore, substantial efforts have been carried out to obtain differently sophisticated polymeric compartments that mimic cells and organelles, in terms of their membrane properties (e.g. permeability vs. non-permeability) for inducing biological pathways or substituting the lack of enzymes in cells and tissues.[3, 8, 16-21]

These polymeric vesicles are composed of amphiphilic moieties forming a bilayer structure, the higher molecular weight of the block copolymer with respect to the natural analogous leads to a larger membrane thickness giving a high robustness and flexibility of the membrane. However, it is also accompanied by a decrease in permeability compared to liposomes.[22, 23] Significant contributions have been made to solve this problem. Some of them focus on the creation of vesicle-templated porous nanocapsules with a precise control of pore size and selective permeability.[24-27] Another attractive and useful alternative is the membrane integration of biomacromolecules (enzymes, protein pores, protein channels, etc.) into the polymersomes.[28-34] These biopores and channels enable the construction of highly permeable membranes establishing cell-like communication functions for small molecules (e.g. nutrients and biologically active molecules).[6, 23, 35] Improved cell mimics (artificial and biohybrid vesicles) are viral capsids,[36] nanomotors[37, 38] or proteinsomes.[39-41]

For mimicking cell functions to exchange (macro)molecules as cargo by crossing stimulated membranes, not only the controlled release of small cargo from artificial devices is of interest, but also the uptake procedure of larger cargo by polymersomes is desirable and of importance.[1-15, 42, 43] Thus, control of the mass transport across the membrane is necessary for any application, requiring the precise knowledge of the variation in the permeability for metabolites inside and outside of cellular mimics in a simplified extracellular environment.[10, 44] For example, a controlled release of the encapsulated cargo is required in the field of drug delivery. In this case of triggered-release systems, ideally complete retention of the cargo in the non-triggered state is desirable. Moreover, compartmentalized reaction systems have great potential to improve multistep enzymatic syntheses with mutually incompatible reaction steps by spatial separation of individual enzymatic transformations.[45-54] For this purpose, a selective mass transport of the substrates and the products across the membrane is needed and the rates of unspecific transport of compounds should be as low as possible. Numerous studies focusing on the permeability of vesicular membranes are based on the use of release assays, investigating the retention of the previously encapsulated molecules within a specified time. However, there are crucial issues when using the release assay, which have to be considered (interaction with the membrane, release conditions, loading efficiency etc.). There are only a few published experimental studies of measuring passive and active permeability of polymersomes for small molecules.[27, 55-58]

Previous own studies on cyclic switching of (multi)enzymatic reactions have been focused on pH- and/or temperature-responsive enzyme-loaded nanoreactors based on photo-crosslinked polymersomes (Psomes), hollow capsules and their multicompartments.[49, 50, 59, 60] For most of these reactive enzymes were enclosed into the inner cavity of the polymeric vesicles during their formation process (*in situ* loading).[49, 50, 59, 60] In a more recent work, *post* and *in situ* loading method has been compared.[42] Thus main locations of biomacromolecules are preferentially determinable due to their characteristics, using a highly sophisticated analytical tool named asymmetrical flow field-flow fractionation (AF4).[42] Summarizing AF4 study for *post* loading swollen Psomes, lower amounts of larger nanoparticles, especially protein mimics and biomacromolecules between Ø of 10-15 nm, can successfully cross the Psomes membrane reaching the lumen during the *post* loading process. Smaller soft and solid nanoparticles (Ø ≤ 7 nm) can be *post* loaded in the Psomes lumen at slightly lower degree as found for *in situ* loaded nanoparticles. It also defines membrane crossing of particles whether particles can also be integrated into the membrane.[42]

From these published observations there are arising following scientific challenges for crossing swollen Psomes´ membrane via a *post* loading approach for the construction of complex artificial organelles outlining the potential of asymmetrically bioactive functionalization of Psomes: First, is there a chance to integrate proteins in Psomes membrane which show non-releasing properties from neutral to slight acidic medium? Second, can this membrane-integrated protein be used as docking platform for other bio(macro)molecules from outside to the lumen of Psomes. This would allow us for postulating the pH-dependent main location of docked bio(macro)molecules at the outer collapsed membrane (pH 8) or in the lumen of swollen pH-responsive Psomes (pH 6). In this context, a further challenge is to develop an optical method which can monitor the location of the integrated protein and the pH-dependent docking process of bio(macro)molecules within and on Psomes. Thus, the aim of the study was to establish pH-stable avidin-loaded polymersomes (Avidin-Psomes) for undergoing pH-dependent docking process of biotinylated (bio)macromolecules through the binding pockets of avidin. Monitoring of the main locations of docked (bio)macromolecules in and on Psomes was possible through the use of fluorescence resonance energy transfer (FRET) experiments. With this approach, the realization of artificial organelles with the potential of asymmetric peptide/protein functionalization (Scheme 1) become accessible

For the purpose of this study, AF4 is used to investigate the structural characteristics of Avidin-Psomes (size, mass, shape, and density; avidin 66 kDa). Results from AF4 and fluorescence spectroscopy enable the prediction of avidin´s loading efficiency and its main location (inside, lumen, outside) as well as its release under different conditions was compared by *in situ* and *post* loading.[42] Avidin offers the possibility of its subsequent functionalization with different biotinylated compounds,[61, 62] thus expanding the loading characteristics of pH-stable Avidin-Psomes (Scheme 1). Subsequently, fluorescent Avidin-Psomes, with integrated Alexa-Fluor 488 labeled avidin, was used in FRET experiments to study the permeability or uptake of Psomes membrane against a broad range of biotinylated (macro)molecules (different molecular structures, sizes and shapes) at different conditions (pH and diffusion time) (Figure 3 and 4). This study together with the previously published work,[42] can establish a superb, sophisticated and general approach to assess the permeability of Psomes and extrapolate it to other types of responsive vesicles and hollow capsules.

.

DOCKING OF BIOTINYLATED (MACRO)MOLECULES IN THE MEMBRANE AND LUMEN
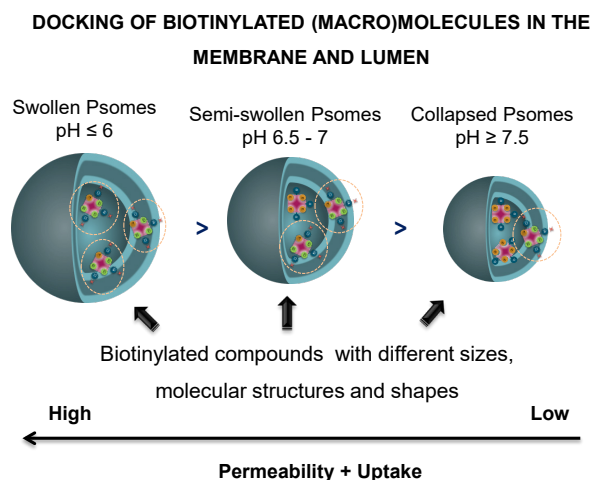
SCHEME 1. Docking regulation of biotinylated biomolecules using by avidin loaded polymersome (Avidin-Psomes) with pH-responsive membrane, regulated through the use of pH-stable Avidin-Psomes.

RESULTS AND DISCUSSION

Formation and characterization of avidin-loaded polymersomes (Avidin-Psomes). To establish above-mentioned aims, empty Psomes and Avidin-Psomes (Figure 1) were fabricated by the self-assembly of BCP (block copolymer) using the so-called pH switch method previously published.[42, 60, 63] Once the Psomes are obtained, they are crosslinked for 3 min of UV irradiation, if not otherwise mentioned, to obtain robust and pH-stable polymeric vesicles (Figure 1 and Table 1).[42, 43, 60, 63, 64] *In situ* and *post* loading method was used to fabricate Avidin-Psomes. *In situ* loading describes the encapsulation of cargo during the formation of Psomes, while *post* loading implies the encapsulation and/or interaction of cargo by/with Psomes after their formation (Figure 1).[42, 60, 65] More details about the preparation and characterization for empty Psomes and Avidin-Psomes are available in Supporting Information (SI).

Cross-linking avoids the typical disassembly of pH-responsive Psomes membrane upon the application of acidic pH stimulus. Moreover, cross-linked empty Psomes and unlabeled Avidin-Psomes (Figure 3 and 4) exhibit enhanced mechanical stability and potentially endless switching on and off membrane permeability by pH cycles (Figure S2). There are nearly differences in the cyclic pH-switches at pH 6.0 (swollen state ~ 150 nm) and pH 8.0 (shrunken state~ 92-98 nm) in presence and absence of avidin for Psomes (Figure S2 and Table 1). Furthermore, avidin´s presence ($\varnothing$ 11 nm; Figure S12) in Avidin-Psomes outline slightly larger diameters and thicker membrane thickness compared to reference, empty Psomes (Table 1). This is similar as found in another study with membrane-

integrated enzyme in Psomes.[42] Results from cryo-TEM images (Figure S21 and Table 1) slightly indicate the presence of membrane-integrated avidin in Avidin-Psomes through *in situ* loading method. Moreover, *in situ* loaded avidin in Avidin-Psomes outline the same collapsed and swollen Psomes membrane states as found for the reference, empty Psomes (Figure S2): collapsed membrane at pH 8 and completely swollen membrane at pH 6.

Avidin location in Avidin-Psomes. The architecture of Psomes offers different locations for the presence of any smaller and larger (macro)molecules (e.g. proteins or peptides): (i) external surface for the attachment of (macro)molecules, by chemical modification of the hydrophilic polymer block or another kind of interaction, (ii) the membrane for insertion of hydrophobic (macro)molecules, (iii) the inner cavity or lumen for encapsulating hydrophilic (macro)molecules. In our study, we aim to postulate the possible locations of avidin in Avidin-Psomes triggered by the combination of loading method (*in situ* and *post*) and purification step (dialysis and hollow fiber filtration (HFF)) (Figure 1). The loading efficiency of dye-labeled avidin through conjugation of biotin-FITC, in each Avidin-Psomes was quantified by fluorescence spectroscopy. Before the study of the possible locations in Avidin-Psomes (Figure 1: (**1**) outer, (**2**) hydrophobic membrane, (**3**) inner, hydrophilic surface, (**4**) lumen and (**5**) free) can be started, a pH-dependent purification step of *in situ* and *post* prepared Avidin-Psomes is crucial. Therefore, dialysis (low shear forces) and hollow fiber filtration (HFF) (high shear forces) were compared as purification methods (Figure 1) to identify the most suited Avidin-Psomes with well distributed avidin biomacromolecules within the locations **1-4** (Figure 1). Details about the fabrication of FITC-labeled Avidin-Psomes are presented in the SI. As can be seen in the Figure 1, since the protein on the surface might interact with the PEG chains (more available; easier to remove) or closer to the membrane (more retained; difficult to remove), a potential intermediate location **1+2** has been assumed. It is not possible to expect that after purification, independent on the used method, some positions are totally eliminated, as it will be explained in more detail later.

Loading efficiency of FITC-labeled avidin in Avidin-Psomes after pH-dependent dialysis and HFF purification is presented in Table 1. Both purification methods were carried out using 1 mM PBS at pH 8, 7 or 6. One of the main differences in the used purification methods is the applied shear force with dialysis leading to a significantly lower shear forces compared to HFF (Figure 1). Thus differences in the loading efficiency are expected, since upon dialysis only free or loosely attached avidin is removerd whereas HFF also removed avidin integrated in the membrane.

AVIDIN-LOADED POLYMERSOMES THROUGH IN-SITU AND POST-LOADING
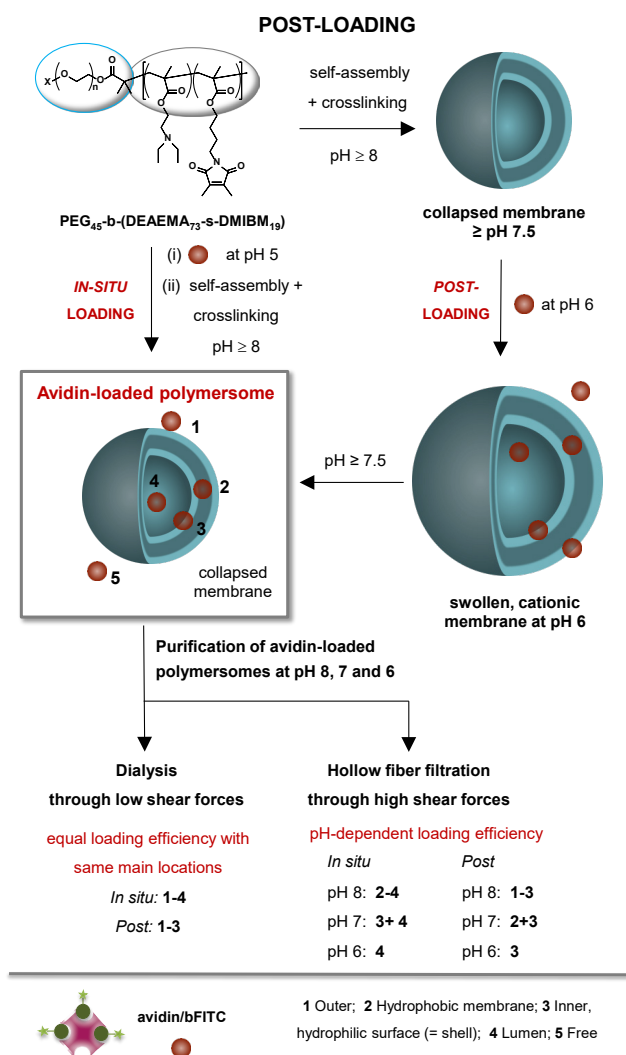
FIGURE 1. General approach for avidin-loaded polymersomes (Avidin-Psomes). Conditions: 1 mg BCP/mL + 0.1 mg/mL avidin/bFITC for Avidin-Psomes. Self-assembly using the pH switch method and crosslinking for 3 min. Postulation of avidin´s locations after each used purification method is also presented (bottom). In the case of dialysis, only free avidin is removed, however, using HFF, avidin anchored in the membrane and outer shell could be removed in the semi or fully swollen state.

For the combination *in situ* loading and dialysis the difference in loading efficiency is negligible despite the use of different pH values during the dialysis. At lower pH, even if the Avidin-Psomes are open (pH 6) or semi-open (pH 7), avidin release is not observed. Thus, mainly the free avidin (location **5**) is removed, while residual avidin can be inside, in the lumen, anchored in the membrane and even on the surface (locations **1-4**).

In case of *post* loading and dialysis, a higher loading efficiency (about 46%) for three different pH values is observed compared to the combination *in situ* loading and dialysis (about 26%) (Table 1). Thus, through the *post* loading the locations **1** and **2** for avidin can be increased in the swollen state (pH 6,

cationic membrane) due to unspecific interactions, improving the loading efficiency. However due to the size of avidin, a penetration of the membrane towards locations **3** and **4** is unlikely, so only the outermost locations are postulated. Previous studies corroborate this hypothesis.[46, 66] It could be an important aspect for future applications. Nevertheless, independent of the loading method the purification method "Dialysis" is not suited to separate preferentially adsorbed avidin biomacromolecules on Psomes outer surface (location **1**) despite the presence of cationic repulsive forces between cationic avidin (isoelectric point ~ 10: highly positive charge density) and cationic Psomes at neutral and acidic conditions. Other strong noncovalent forces (e.g. H-bonds between hydroxy of sugar and PEG shell of Psomes) must overcome cationic repulsive charges due to the presence of sugar units in the outer surface of avidin.[67-70]

The use of HFF purification method for *in situ* and *post* loading method (Table 1) emphasizes the desired pH-dependent separation effect of avidin biomacromolecules from outside (location **1**) to inside (locations **2-4**) (Figure 1, bottom right). By *in situ* loading for Avidin-Psomes purified at pH 8 (collapsed state), the loading efficiency is 7.2%. Thus, free avidin (location **5**) and almost on the surface (location **1**) is removed, while remaining avidin biomacromolecules in Avidin-Psomes are available at locations **2-4** (Figure 1: maybe residual location **1+2**). At pH 7 (semi-swollen state), loading efficiency is reduced to 4.3%.

Therefore, the release of avidin anchored in the membrane or near the surface is postulated and locations **3-4** remain. Finally, loading efficiency is further reduced to 3.5% at pH 6 (swollen state). Here we postulate that avidin is mainly located in the lumen (location **4**). By *post* loading for Avidin-Psomes, results are similar to *in situ* loading (Table 1), with a slight exception at pH 6. For the slight exception it is postulated that using *post* loading leads to a slightly larger amount of attached avidin in the membrane than in the case of *in situ* loading; this is in analogy to previously published data with *in situ* and *post* loaded myoglobin and protein mimics by swollen Psomes.[42] Furthermore, in case of *in situ* loading, avidin is probably mainly in the lumen and a small percentage in the membrane at pH 6.

In order to achieve high differentiation of the locations of avidin at applied pH values (pH 8, 7 and 6) (Table 1), the *post* loading seems to be the more appropriate method. *Post* loading combined with HFF purification is easier, versatile and more successful. However, in this work we are interested in a permeability study having a strong differentiation between surface-attached and lumen-located biomacromolecules in the Psomes. This requires a low amount of avidin in the membrane. Therefore, the combination *in situ* loading method with HFF as a purification method was chosen due to the main location of avidin inside the vesicle and the low percentage of attached avidin in the membrane for the final study on the permeability of Avidin-Psomes (Figure 3 and 4). This fact was previously already been corroborated, the activity of enzymes

can be regulated by our pH sensitive polymersomes, proving its location mainly in the lumen. Obviously, a certain percentage of enzymes has also been observed in the membrane according to the enzyme or protein characteristics used (Figure S23: further details for identifying protein´s location in Psomes).[42, 60, 65] This pre-consideration further strengthens to carry out the final permeability study on Avidin-Psomes. Further support for the postulation of avidin´s locations in Avidin-Psomes was validated by AF4.

TABLE 1. Average diameter and thickness by dynamic light scattering and cryo-TEM at pH 8. Loading efficiency using different loading and purification methods.

		Empty-Psome	Avidin-Psome* *In situ* loading	Avidin-Psome* *Post* loading
Size (nm)[a]	pH 8	96.9 $\pm$ 0.1	92.5 $\pm$ 1.3	97.5 $\pm$ 0.2
	pH 6	150 $\pm$ 0.1	148.3 $\pm$ 1.0	146.4 $\pm$ 0.1
Size (nm)[b]		74.5 $\pm$ 13	82.0 $\pm$ 19	-
Membrane thickness (nm)[b]		16.0 $\pm$ 2.3		18.3 $\pm$ 3.9
		Avidin- Psome* *In situ* loading	**Avidin- Psome*** *Post* loading	
Loading efficiency (%) using dialysis	pH 8	26 $\pm$ 8	47 $\pm$ 5	
	pH 7	26 $\pm$ 9	45 $\pm$ 7	
	pH 6	25 $\pm$ 9	44 $\pm$ 5	
Loading efficiency (%) using HFF	pH 8	7.2 $\pm$ 2.2	7.5 $\pm$ 3.6	
	pH 7	4.3 $\pm$ 1.0	4.3 $\pm$ 1.2	
	pH 6	3.5 $\pm$ 0.5	2.8 $\pm$ 0.5	

[a] Average diameter by dynamic light scattering at pH 6 and 8. [b]Cryo-TEM of Empty-Psome and avidin loaded crosslinked polymersome (*In situ* loading) (Figure S21). All samples were prepared 1 mg BCP/mL + 0.1 mg/mL avidin and 3 min crosslinking time.
Loading efficiency was calculated using fluorescence spectroscopy (λ_{exc} = 493 nm, λ_{obs} = 518 nm). All samples were studied at 0.25 mg BCP/mL in 10 mM PBS at pH 7.4. The experiments were carried out by triplicate.

Structural Parameters of Avidin-Psomes Investigated by Asymmetrical Flow Field-Flow Fractionation (AF4). To validate the afore-mentioned possible avidin´s locations in Avidin-Psomes, an in-depth characterization has been carried out by AF4 coupled to static and dynamic light scattering.[42] Using these analytical tools two goals can be achieved: i) the separation and quantification of the non-encapsulated avidin from Avidin-Psomes and ii) the evaluation of the conformation of the Avidin-Psomes assemblies in dependence of the loading method, *in situ* or *post*. Furthermore, the main and/or minor location of avidin in Avidin-Psomes (Locations **1-4** in Figure 1) should provide significant insight into the tailoring of loading parameters. To evaluate changes in Avidin-Psomes elution behavior and shape, empty Psomes were precisely characterized before the loading experiments started.
For the AF4 study no purification step was performed to *in situ* and *post* loading solution, thus free protein and Avidin-

Psomes are coexisting in the sample solution. In contrast to HFF purification, the forces applied during AF4 separation are too weak to break the interaction between the vesicle surface and the cargo (similar to dialysis); some interaction with the membrane of AF4 might be possible as well. First of all, we developed an adequate protocol to separate free avidin (66 kDa, $\varnothing$ 11 nm (Figure S12)) from Avidin-Psomes possessing different sizes. Thus, *in situ* and *post* prepared Avidin-Psomes were used, and empty Psomes was applied as reference. Conditions for the fabrication of Avidin-Psomes and Psomes are 0.5 mg BCP/mL with/without 0.05 mg/mL avidin in 1 mM PBS at pH 8 (Further details in SI). To optimize the fractionation, baseline separation between Avidin-Psomes and avidin is essential and is monitored by concentration sensitive UV and RI signals (Figure 2, bottom-left).

Unfortunately, a direct quantification of loaded avidin is not possible. The calibration of the UV signal area with concentration series of the individual protein enables us to quantify free avidin and to calculate the amount of loaded protein by Psomes (Figure S3). Using this protocol, an encapsulation efficiency $\geq$ 88 % is determined. This encapsulation efficiency only considers unpurified samples compared with the data obtained by fluorescence study (Table 1) where dialysis was used to obtain purified samples. The high loading efficiency can be explained due to a possible interaction between avidin and the membrane of AF4 device, which decreases the free avidin peak giving higher percentage of encapsulation. Nevertheless, this proves a high interaction between avidin and Psomes under very low shear forces in AF4 study.

Yet, the structural parameters are the most valuable information extracted from this AF4 study. For hard sphere in a good solvent ν = 0.33 is expected corresponding to 3D fractal object. Though, this value is additionally strongly depending on the nature of particles surface. The conformation plots of the empty Psomes, determined at pH 8, indicate uniform particle conformation close to sphere independently on the applied pH. Indeed, the study of the Psomes membrane conformation after enzyme loading shows clear differences depending on the type of protein and loading approach.[42]

The scaling parameter is very similar for both loading methods; both curves are shifted to higher radii after loading (same molar masses but higher radius). This indicates that the conformation of empty Psomes is practically unchanged after the loading (Figure 2, top-left). In the molar mass region of the main Psomes fraction (up to 60 kDa) R_g/R_h is close to 1, typical for hollow spheres (Figure 2, top-right). With increasing molar mass, aggregation of Psomes can happen and the ρ parameter increases, the spherical structure is not present anymore, more aggregates (multiple Psomes together) with complex conformation are formed. Slight changes of the membrane are observed after in situ loading (ν = 0.42 in comparison to ν = 0.44 Empty-Psome). These might be due to the incorporation of avidin into the membrane that creates a small deformation in the membrane in *in situ* loading in comparison with *post* loading. Accordingly, the corresponding apparent density decreases clearly (Figure 2, bottom-right) in both cases

(*in situ* and *post* loading). It confirms that avidin is incorporated into the membrane Psomes, location **2**. The same interpretation has been confirmed by DLS and cryo-TEM (Table 1), leading to the conclusion that avidin does not lead to significant membrane, diameter or shape changes, probably being too small.
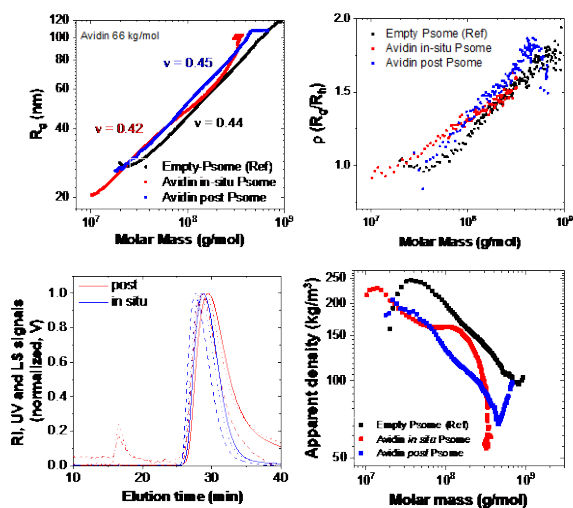
FIGURE 2. Conformation plot of polymersome measured at pH 8 indicating uniform particle conformation with well-defined surface. The inset shows the apparent density calculated according to molar mass (M_w) and radius (R_g) with the assumption of spherical shape. Conditions: 0.5 mg BCP/mL + 0.05 mg/mL avidin. AF4 fractograms of polymersomes. (Top-left) Conformation plot of polymersomes: pure, *in situ* loaded, and *post* loaded with avidin. (Top-right) R_g/R_h dependency on the molar mass. (Bottom-left) Static light scattering, UV and RI signal after AF4 separation of two systems: free protein and loaded- Psomes. (Bottom-right) Apparent density calculated for polymersomes: pure, *in situ* loaded, and *post* loaded with avidin.

Permeability study on pH-responsive Avidin-Psomes using a FRET effect. To deepen our understanding of the permeability of the Avidin-Psomes, in analogy to our previous *post* loading of nanoparticles (e.g. proteins and protein mimics) through swollen pH-responsive Psomes,[42, 43] fluorescence resonance energy transfer (FRET) effect was implemented in Avidin-Psomes through the integration of bioconjugates (BC-HABA), consisting of Alexa Fluor 488-labeled avidin (AAF-488) and HABA (Figure 3A). The functional principle of a FRET experiment (Figure 3A) is that the fluorescence of the Alexa Fluor-488 dye is quenched by FRET through the addition of the quencher dye HABA. When biotinylated compounds are added to the reaction mixture, then the HABA is displaced by them, resulting in an increase in fluorescence (Figure 3A).[71]

Thus, this effect was used to study the permeability of collapsed and swollen Psomes membrane against a broad range of biotinylated (macro)molecules (different molar structures, sizes and shapes) at different pH conditions. The permeability

of Psomes membrane can be triggered by: (a) crosslinking density; (b) pH and ion composition of solution; (c) block copolymer composition for Psomes fabrication; and (d) size-, charge- and shape of biotinylated (macro)molecules. Here, the permeability has mainly been studied in the context of pH-trigger and defined diffusion time.

To carry out the permeability study on Avidin-Psomes, conditions were chosen that avidin is preferentially located in the lumen of Avidin-Psomes (location 4) and only minor amounts of avidin are located in the membrane (preferred locations 2 + 3). The uptake of biotinylated compounds, presented later in state 1, 2 and 3, occurs through avidin-biotin conjugation process (Figure 4).

Probing the function of FRET, control experiments were carried out to validate the stability of BC-HABA at different pH (more details in the SI, Figure S6-S12): (a) titration of free AAF-488 with HABA; (b) titration of BC-HABA with biotin; (c) pH dependency of BC-HABA. Thus, the FRET effect was clearly proven. A small pH dependency was noted. For this reason, all fluorescence measurements are carried out at the same pH. In addition, the number of displaced HABA by biotin, or later by biotinylated (macro)molecules, cannot be estimated exactly. Therefore, the results validated have to considered to be just qualitative (e.g. Figure S10 or Figure 4).

The approach of BC-HABA loaded Psomes (HAAP) (Figure 3A) is presented in detail in SI. HAAP is always used in the following presented results (Figure 3D and 4) for clarifying the potential use of Avidin-Psomes in pH-dependent *post* loading processes. Figure 3B presents the final preparation step of HAAP through the stepwise titration with HABA (0-25 μg/mL) in presence of AAF-488-loaded Psomes (AAP, Figure 3A). Finally, the addition of 25 μg HABA to AAP was chosen as the optimal concentration for preparing HAAP with excess HABA needed for our FRET experiments (Figure 3D and 4).

For studying the permeability of pH-responsive Avidin-Psomes one obligated requirement is to determine the key pH values that define different opening states (collapsed, semi-swollen or swollen state). Previously, a detailed work was established about pH* (semi swollen state, half open) for our pH-responsive Psomes.[65, 72] This value is around 6.3 in Millipore water and using 1 mg BCP/mL. However, it is important to study this key parameter under the right conditions. For all permeability experiments, concentration of Psomes is $C_{avidin-Psome}$ = 0.25 mg BCP/mL in 1 mM PBS and in presence of HABA (C_{HABA} = 1 mM, 1 mM PBS) (Figure 3C). The pH* value is 6.9 (Figure 3C) which is shifted to higher values compared to the conditions previously studied.[65, 72] This shift to higher value is caused by the presence of buffer and HABA; a typical behavior when ionic solutions are present in Psomes solution.[65, 72] Therefore, we defined pH 6 (swollen state), pH 7 (semi-swollen state) and pH 8 (collapsed state).

The first permeability experiment of HAAP with a short bPEGNH2 (500 Da) at different pH (5.5, 6, 6.5, 7 and 7.5) (Figure 3D) was carried out to test the key parameters for pH-dependent permeability of Avidin-Psomes. At pH 5.5, 6 and 6.5 there is no difference, while HAAP is already swollen in

this pH range (Figure 3C). At pH 7, the semipermeable state is identified, while at pH 7.5 HAAP is suited for starting surface-driven interaction at location **1+2** (= just before to start membrane swelling to lower pH; Figure 3C).

In this study HAAP sample (Figure 3A) purified at pH 8 was used, residual avidin after purification step in the location **1+2**

was already postulated previously (Figure 1). Thus, it is reasonable that a slightly increasing fluorescence is visible at pH 7.5 due to docking process at location **1+2**. This thoroughly implies that Psomes with collapsed membrane still exist at pH 7.5, and no obvious permeability of Psomes membrane is present at this pH value.
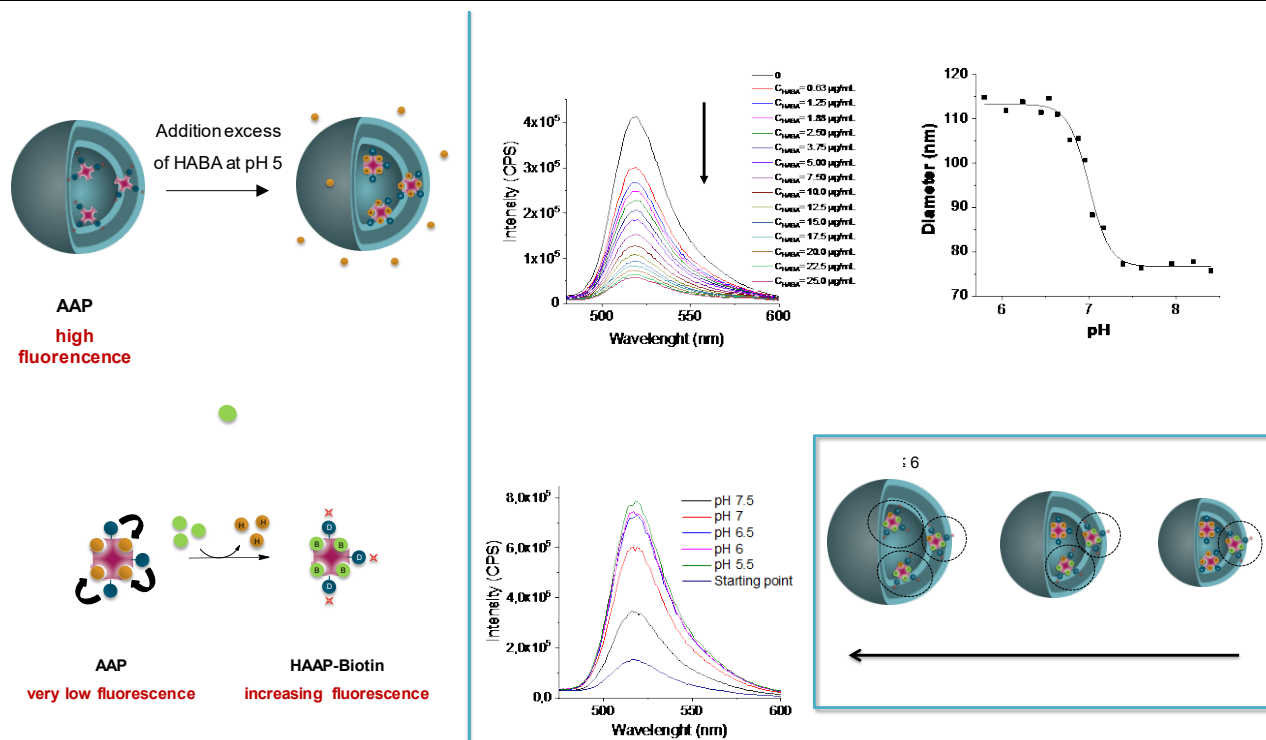
FIGURE 3. General approach for the establishment of membrane diffusion of biotinylated compounds through the fabrication of BC-HABA-loaded Psomes (HAAP). (A) Fabrication of HAAP using *in situ* loading of AAF-488 loaded Psomes (AAP) and theoretical point of view on FRET effect. Conditions: 1 mg BCP/mL + 0.1 mg/mL Alexa Fluor-488 conjugated avidin (AAF-488). Self-assembly using the pH switch method and crosslinking for 3 min. The sample was purified using HFF against 1 mM PBS at pH 8 (8.7 $\pm$ 0.8 % encapsulation efficiency). (B) Titration of AAP using different HABA concentrations at pH 6 monitored by fluorescence intensity (λ_{exc} = 317 nm; λ_{obs} = 516 nm). (C) pH-dependent DLS measurements– determination of pH* (half power of Psome swelling) of HAAP with 0.25 mg BCP/mL in 1 mM PBS in presence of excess HABA. (D) First permeability study on short bPEG-NH$_2$ (b1, 500 Da, Table 2) at different pH for validating the use of FRET effect in HAAP.

TABLE 2. List of the used biotinylated (macro)molecules used.

Samples	Shape/Type of biomolecules/biotin groups
b1 bPEGNH2 500 Da	Linear/neutral, PEG/ mono
b2 bPEGNH2 3kDa	Linear/ neutral, PEG/mono
b3 bPEGNH2 5kDa	Linear/ neutral, PEG/mono
b4 bPEGNH2 10kDa	Linear/ neutral, PEG/mono
b5 bTAT2kDa	Linear/cationic, peptide/mono
b6 bCPP3kDa	Linear/ cationic, peptide/mono
b7 bPPI43kDa	Spherical/ cationic/mono
b8 bHRP44kDa	Spherical/cationic, enzyme/penta
b9 bHA7kDa	Linear/anionic/mono
b10 bHSA66kDa	Spherical/ anionic, protein/mono
b11 bGOx160kDa	Spherical/ anionic, enzyme/penta
b12 bCAT240kDa	Spherical/ anionic, enzyme/hexa
b13 bPNIPAM5kDa	Linear/ neutral, polymer/ mono
b14 bPNIPAM2.5kDa	Linear/ neutral, polymer/ mono

Abbreviations: PEG = poly(ethylene glycol); PPI = poly(propylene imine); HRP = horseradish peroxidase; HA = hyaluronic acid; HSA = human serum albumin; GOx = glucose oxidase; CAT = catalase; PNIPAM = poly-(N-isopropyl acrylamide)

Summarizing the previous results of short bPEGNH2 (b1; Table 2) avidin is anchored in the membrane and a small amount attached at the outer surface, identifying avidin´s location **1** and **2** (Figure 1). This should allow us to postulate some pH-dependent permeability and docking characteristics. The final pH-dependent permeability study on HAAP (Figure 4) was carried out with fourteen biotinylated (macro)molecules (b1 – b14) possessing different sizes, structures, charges and shapes (Table 2 and Table S6). The vast majority of b1 – b14 is commercially available, except b6, b7, b9, b10, b13 and b14 which have been synthesized and characterized (Further details in the SI). Before designing the final permeability experiment (Figure S26), the HABA assay was performed to quantify the biotin groups in b1 – b14 (Table 2). It is important to note that not all compounds are monobiotinylated: b8, b11, b12 (Table 2). However, in the final study (Figure 4), the same number of biotin groups was added in each case to allow a comparison and a better conclusion of their permeability characteristics.

The results of final FRET experiment for the determination of permeability characteristics of b1 – b14 against HAAP is presented in Figure 4 (bottom). To seriously discuss the results b1 – b14 were analyzed at three different pH values (6, 7 and 8) after 8 h incubation in presence of HAAP at which pH values present three different states of HAAP: State I – Collapsed at pH 8; State II- Semi-swollen at pH 7; State III- Swollen at pH 6. After the incubation time, all samples were analyzed at pH 6 avoiding interferences of pH dependence (Figure 4, bottom). Thus, the results of our study can be divided into three states for final discussion:

In State I, the membrane is practically impermeable in all cases, and there is no difference between b1 – b14 studied. The residual signal ($\leq$ 15 %) obtained is due to the presence of a small amount of avidin in the (outer) membrane, location **2** or even maybe residual location **1 + 2** (Figure 1, Figure S23: protocol for identifying protein locations). Thus, in the collapsed state, b1 – b14 can interact with a small amount of avidin at location **1** and **2**. However, the uptake of the biotinylated compounds is very low in all cases, indicating no permeability capacity for crossing the HAAP membrane to avidin locations 3 and 4 and also points to only a low amount of avidin on the surface.

In state II, the uptake capacity (2-17 %) increases slightly, then locations **2** and **3** (Figure 4) could become more accessible. This increase is lower (< 5%) in the case of b5, b13 and b14. In the case of b5 (bTAT), Psomes are partially positively charged at pH 7 and can suppress possible interaction with cationic bTAT. Something similar could happen with polymers b13 and b14 (bNIPAM), their H-bond-active structure can interact more with PEG shell of HAAP than with its membrane.

Finally, in State III, all biomacromolecules (b8, b11 and b12), except b10, show a doubling of their uptake ability, compared to state II. This corroborates an increase in the permeability of the membrane and a possible interaction with location **4** (Figure 4). Considering the afore-mentioned size-, charge- and shape-dependent permeability parameter for biotinylated (macro)molecules, it seems that only the size could be the determining permeability parameter. Taking into account the size (Table S6), larger ($\varnothing$ 6.7 – 15.9 nm) biomacromolecules such as bHRP (b8, 44 kDa), bHSA (b10, 66 kDa), bGOx (b11, 160 kDa) and bCAT (b12, 240 kDa) show an increase, but much lower in comparison with the rest (b1 – b7, b9, b13 and b14; Figure 4). In the swollen state, these biomacromolecules (b8, b10-b12) cannot cross the vesicle membrane to the lumen. However, the avidin at location **3** (Figure 4) is maybe more accessible for them. The rest of the biomolecules (b5, b6 and b9) are able to penetrate the membrane towards to the lumen (location **4**). The glycodendrimer bPPI (b7, $\varnothing$ 6.8 nm, 40 kDa) does not follow the described trend for the biomacromolecules. Its ability to reach location **4** is similar to the behavior observed for small (bio)molecules (b1-6 and b9). Known from a previous study that glycodendrimer b7 is suited to cross the membrane.[43] Generally, the *post* loading approach for Avidin-Psomes leads to a successful loading of all kinds of biotinylated (macro)molecules.
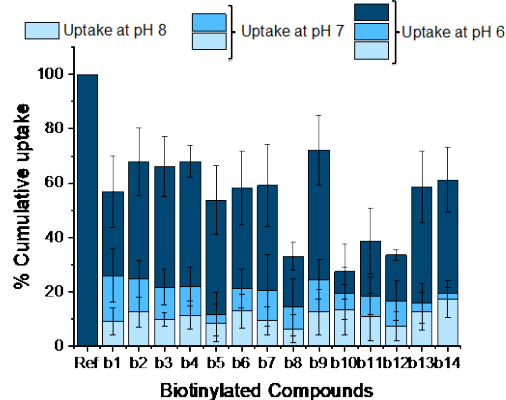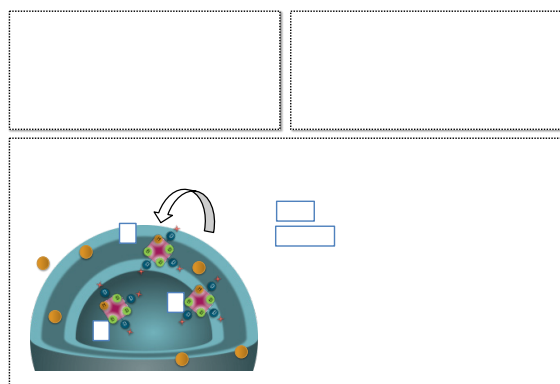
FIGURE 4. General approach for the establishment of membrane diffusion of biotinylated compounds determined through the validation of FRET experiments. Conditions: 0.25 mg BCP/mL + 0.025 mg/mL AAF-488 (8-10 % encapsulated in HAAP). Ref 100% = AAF-488-loaded Psomes (AAP) (Figure 3). The used calculation method to obtain the cumulative uptake is presented in the SI.

Thus, this study emphasizes an alternative to the *in situ* loading process of Psomes. Moreover, this thoroughly allows the additional uptake of compounds of interest by the fully swollen Psomes within the membrane (location 2), inside the lumen (locations 3 and 4). Finally, the lower permeability of biomacromolecules (b8, b10-b12) also implies that *in situ* loaded avidin in HAAP will not be released from the lumen to outside.

EXPERIMENTAL SECTION

Fabrication of AAF-488 in situ loaded Psomes for final FRET experiments. For AAF-488 *in situ* loaded Psomes (AAP in Figure 3A) the method of Gräfe et al.[60] has been adopted and modified for AAF-488. 16 mg of BCP were dissolved in 14.5 mL of 10 mM hydrochloric acid (pH 2), after complete dissolving this solution was passed through a 0.2 μm nylon filter. Then, in a solution of 13.5 mL (1mg BCP/mL 0.01 M HCl) the pH was adjusted around pH 5 by adding 1N NaOH slowly, and then, 1.5 mL of filtered solution of AAF-488 (1.5 mg of Alexa Fluor-488 labeled avidin (AAF-488) + in 1.5 mL of 1 mM PBS; dissolving AAF-488 1 day before) were added. Finally, to induce the self-assembly process for

AAF-488 *in situ* loaded Psomes, deprotonation of the tertiary amine moieties is performed by simply increasing the pH to a basic state (pH 8). After 3 days of stirring, the final polymersome structure is formed. The final block copolymer concentration must be of 1 mg/mL and the AAF-488 concentration of 0.1 mg/mL. The obtained AFF-488 *in situ* loaded Psomes solution was filtered using 0.8 μm nylon filter and was placed in the UV chamber and irradiated for 3 min to obtain robust and mechanically stable Psomes. The resulting solution was cleaned from non-enclosed protein using HFF. For HFF separation the sample was cleaned against 1 mM PBS buffer at pH 8 or at pH 6. The transmembrane pressure is kept at 130 mbar during the whole process until extracting the total sum of 150 mL volume.

Permeability study of short bPEGNH2 (500Da) on HAAP through FRET experiment at different pH values. A solution of AAF-488 loaded Psomes [1 mg BCP/mL and 0.01 mg AAF-488/mL; V_{total} = 5 mL, crosslinking time = 3 min, purified by HFF at pH 8 was prepared and their pH was adjusted to pH 6 for the addition of 6.1 μL of HABA (fresh solution, 10 mM). The sample was stirred for 1 h. The fluorescence intensity should be checked before and after adding HABA in order to check a right quenching of Alexa Fluor-488 in AAF-488 *in situ* loaded Psomes. Subsequently, 0.25 mg/mL BC-HABA-loaded Psomes (HAAP, Figure 3) solution were prepared in 1 mM PBS at different pH (7.5, 7, 6.5 and 6). Later, the short bPEGNH2 (500 Da; Table 2: b1) was added to all different mentioned conditions. After 4 h of incubation, all samples were adjusted at pH 6 and the fluorescence intensity was checked (λ_{exc} = 317 nm). All samples were studied at 0.25 mg BCP/mL and the experiments were carried out by triplicate.

Permeability study of biotinylated (macro)molecules on HAAP through FRET experiment at different pH values. For a solution of HAAP (0.25 mg BCP/mL, V_{total} = 20 mL; Figure 3A) the pH was adjusted to pH 6 and then, 120 μL of HABA (fresh solution, 1 mg/mL) was added. The sample was stirred for 2 h. The samples before and after adding HABA were used as reference (triplicate) to check the right quenching of AAF-488 in HAAP (100 μL per well). Subsequently, 0.25 mg BCP/mL for BC-HABA loaded Psomes (HAAP) solution were prepared in 1 mM PBS at different pH (8, 7 and 6) and setting it in a 96 well plate (100 μL per well). Later, the different biotinylated (macro)molecules were added. After 8 h of incubation, all samples were adjusted to pH 6, adding 100 μL of 10 mM PBS at pH 6 per well to study the fluorescence intensity (Design of FRET experiment in Figure S22 and used concentration of all biotinylated (macro)molecules presented in Table S5). All samples were studied by fluorescence microscopy using a microplate reader. λ_{exc}: 488 nm (Figure S22). The experiments were carried out by triplicate and by duplicate in each plate. The used calculation method to obtain the cumulative uptake is presented in the SI (Section 10).

CONCLUSIONS

This study provides deeper insights into the *in situ* loading and *post* loading of photo-crosslinked Psomes with avidin (Avidin-

Psomes). Most studies on the loading of proteins by Psomes mainly consider the final validation of loading efficiency,[73, 74] but not the verification of (i) (macro)molecules locations within the molecular structure of Psomes itself and (ii) the consideration of the structural parameters of Psomes in presence and absence of loaded proteins.[29, 75] This work contributes to a deeper study on the possible avidin locations in our Avidin-Psomes and which of them are accessible depending on the pH and the (structural) characteristics of biotinylated (macro)molecules used. The results from the analytical tools, AF4 and fluorescence spectroscopy, using FRET effect, thoroughly support us to formulate one dominating permeability parameter, the size, for the *post* loading of Avidin-Psomes. Extracted from the permeability study (Figure 4), (macro)molecules (Mw ≤ 40 kDa) can be captured in the lumen and in the membrane (locations **2 - 4**) by a *post* loading method. Although the success is lower for larger biomacromolecules (Mw ≥ 40 kDa), the possibility of their incorporation into the membrane is nevertheless shown (location **2 + 3**). This emphasizes a new and valuable tool to prepare artificial organelles with asymmetrically addressable functional units through the biofunctionalization of a new kind of pH-stable Avidin-Psomes in the collapsed and swollen state. In the near future, protein trapping and surface decoration after *post* loading of Avidin-Psomes and other avidin-loaded polymeric capsules can pave the way of exciting new approaches, for example, in vesicle-based bionanotechnology.

ASSOCIATED CONTENT

Supporting Information

The Supporting Information contains residual experimental descriptions for materials and BCP, Psomes and Avidin-Psomes syntheses, including synthesis and characterization of biotinylated compounds and description for FRET experiments and additional figures for FRET results. The Supporting Information is available free of charge on the ACS Publications website.

AUTHOR INFORMATION
Corresponding Authors. *E-mail: moreno@ipfdd.de (S.M.). *E-mail: applhans@ipfdd.de (D.A.).

Notes. The authors declare no competing financial interest.

REFERENCES

1. Elani, Y.; Trantidou, T.; Wylie, D.; Dekker, L.; Polizzi, K.; Law, R. V.; Ces, O., Constructing vesicle-based artificial cells with embedded living cells as organelle-like modules. *Sci. Rep.* **2018,** *8* (1), 4564.

2. Gaitzsch, J.; Huang, X.; Voit, B., Engineering Functional Polymer Capsules toward Smart Nanoreactors. *Chem. Rev.* **2016,** *116* (3), 1053-1093.

3. Iqbal, S.; Blenner, M.; Alexander-Bryant, A.; Larsen, J., Polymersomes for Therapeutic Delivery of Protein and Nucleic Acid Macromolecules: From Design to Therapeutic Applications. *Biomacromolecules* **2020,** *21* (4), 1327-1350.

4. Ke, W.; Li, J.; Mohammed, F.; Wang, Y.; Tou, K.; Liu, X.; Wen, P.; Kinoh, H.; Anraku, Y.; Chen, H.; Kataoka, K.; Ge, Z., Therapeutic Polymersome Nanoreactors with Tumor-Specific Activable Cascade Reactions for Cooperative Cancer Therapy. *ACS Nano* **2019,** *13* (2), 2357-2369.

5. Lai, M.-H.; Lee, S.; Smith, C. E.; Kim, K.; Kong, H., Tailoring polymersome bilayer permeability improves enhanced permeability and retention effect for bioimaging. *ACS Appl. Mater. Interfaces* **2014,** *6* (13), 10821-10829.

6. Palivan, C. G.; Goers, R.; Najer, A.; Zhang, X.; Car, A.; Meier, W., Bioinspired polymer vesicles and membranes for biological and medical applications. *Chem. Soc. Rev.,* **2016,** *45* (2), 377-411.

7. Pawar, P. V.; Gohil, S. V.; Jain, J. P.; Kumar, N., Functionalized polymersomes for biomedical applications. *Polym. Chem.* **2013,** *4* (11), 3160-3176.

8. Rideau, E.; Dimova, R.; Schwille, P.; Wurm, F. R.; Landfester, K., Liposomes and polymersomes: a comparative review towards cell mimicking. *Chem. Soc. Rev.,* **2018,** *47* (23), 8572-8610.

9. Rodríguez-García, R.; Mell, M.; López-Montero, I.; Netzel, J.; Hellweg, T.; Monroy, F., Polymersomes: smart vesicles of tunable rigidity and permeability. *Soft Matter* **2011,** *7* (4), 1532-1542.

10. Schwarzer, T. S.; Klermund, L.; Wang, G.; Castiglione, K., Membrane functionalization of polymersomes: alleviating mass transport limitations by integrating multiple selective membrane transporters for the diffusion of chemically diverse molecules. *Nanotechnology* **2018,** *29* (44), 44LT01.

11. Simón-Gracia, L.; Hunt, H.; Scodeller, P. D.; Gaitzsch, J.; Braun, G. B.; Willmore, A.-M. A.; Ruoslahti, E.; Battaglia, G.; Teesalu, T., Paclitaxel-Loaded Polymersomes for Enhanced Intraperitoneal Chemotherapy. *Mol. Cancer. Ther.* **2016,** *15* (4), 670-679.

12. Wang, F.; Gao, J.; Xiao, J.; Du, J., Dually Gated Polymersomes for Gene Delivery. *Nano Lett.* **2018,** *18* (9), 5562-5568.

13. Yassin, M. A.; Appelhans, D.; Wiedemuth, R.; Formanek, P.; Boye, S.; Lederer, A.; Temme, A.; Voit, B., Overcoming Concealment Effects of Targeting Moieties in the PEG Corona: Controlled Permeable Polymersomes Decorated with Folate-Antennae for Selective Targeting of Tumor Cells. *Small* **2015,** *11* (13), 1580-1591.

14. Liu, G.; Ma, S.; Li, S.; Cheng, R.; Meng, F.; Liu, H.; Zhong, Z., The highly efficient delivery of exogenous proteins into cells mediated by biodegradable chimaeric polymersomes. *Biomaterials* **2010,** *31* (29), 7575-85.

15. Nomani, A.; Nosrati, H.; Manjili, H. K.; Khesalpour, L.; Danafar, H., Preparation and Characterization of Copolymeric Polymersomes for Protein Delivery. *Drug Res.* **2017,** *67* (8), 458-465.

16. Blackman, L. D.; Varlas, S.; Arno, M. C.; Fayter, A.; Gibson, M. I.; O'Reilly, R. K., Permeable Protein-Loaded Polymersome Cascade Nanoreactors by Polymerization-Induced Self-Assembly. *ACS Macro Lett.* **2017,** *6* (11), 1263-1267.

17. Blackman, L. D.; Varlas, S.; Arno, M. C.; Houston, Z. H.; Fletcher, N. L.; Thurecht, K. J.; Hasan, M.; Gibson, M. I.; O'Reilly, R. K., Confinement of Therapeutic Enzymes in Selectively Permeable Polymer Vesicles by Polymerization-Induced Self-

Assembly (PISA) Reduces Antibody Binding and Proteolytic Susceptibility. *ACS Cent. Sci.* **2018**, *4* (6), 718-723.

18. Moquin, A.; Ji, J.; Neibert, K.; Winnik, F. M.; Maysinger, D., Encapsulation and Delivery of Neutrophic Proteins and Hydrophobic Agents Using PMOXA-PDMS-PMOXA Triblock Polymersomes. *ACS Omega* **2018,** *3* (10), 13882-13893.

19. Wang, G.; Castiglione, K., Light-Driven Biocatalysis in Liposomes and Polymersomes: Where Are We Now? *Catalysts* **2018,** *9* (1), 12.

20. Zhong, Y.; Meng, F.; Zhang, W.; Li, B.; van Hest, J. C. M.; Zhong, Z., CD44-targeted vesicles encapsulating granzyme B as artificial killer cells for potent inhibition of human multiple myeloma in mice. *J. Controlled Release* **2020,** *320*, 421-430.

21. Sun, J.; Mathesh, M.; Li, W.; Wilson, D. A., Enzyme-Powered Nanomotors with Controlled Size for Biomedical Applications. *ACS Nano* **2019,** *13* (9), 10191-10200.

22. Battaglia, G.; Ryan, A. J.; Tomas, S., Polymeric Vesicle Permeability: A Facile Chemical Assay. *Langmuir* **2006,** *22* (11), 4910-4913.

23. Lomora, M.; Dinu, I. A.; Itel, F.; Rigo, S.; Spulber, M.; Palivan, C. G., Does Membrane Thickness Affect the Transport of Selective Ions Mediated by Ionophores in Synthetic Membranes? *Macromol. Rapid. Commun.* **2015,** *36* (21), 1929-1934.

24. Dergunov, S. A.; Kim, M. D.; Shmakov, S. N.; Pinkhassik, E., Building Functional Nanodevices with Vesicle-Templated Porous Polymer Nanocapsules. *Acc. Chem. Res.* **2018**.

25. Kim, K. T.; Cornelissen, J. J. L. M.; Nolte, R. J. M.; Hest, J. C. M. v., A Polymersome Nanoreactor with Controllable Permeability Induced by Stimuli-Responsive Block Copolymers. *Adv. Mater.* **2009,** *21* (27), 2787-2791.

26. Spulber, M.; Najer, A.; Winkelbach, K.; Glaied, O.; Waser, M.; Pieles, U.; Meier, W.; Bruns, N., Photoreaction of a hydroxyalkyphenone with the membrane of polymersomes: a versatile method to generate semipermeable nanoreactors. *J. Am. Chem. Soc.* **2013,** *135* (24), 9204-9212.

27. Wang, X.; Yao, C.; Zhang, G.; Liu, S., Regulating vesicle bilayer permeability and selectivity via stimuli-triggered polymersome-to-PICsome transition. *Nat. Commun.* **2020,** *11* (1), 1524.

28. Bruns, N.; Lörcher, S.; Makyła-Juzak, K.; Pollarda, J.; Renggli, K.; Spulber, M., Combining Polymers with the Functionality of Proteins: New Concepts for Atom Transfer Radical Polymerization, Nanoreactors and Damage Self-reporting Materials. *Chimia* **2013,** *67*, 777-81.

29. Itel, F.; Najer, A.; Palivan, C. G.; Meier, W., Dynamics of Membrane Proteins within Synthetic Polymer Membranes with Large Hydrophobic Mismatch. *Nano Lett.* **2015,** *15* (6), 3871-3878.

30. Kauscher, U.; Holme, M. N.; Björnmalm, M.; Stevens, M. M., Physical stimuli-responsive vesicles in drug delivery: Beyond liposomes and polymersomes. *Adv. Drug. Deliv. Rev.* **2019,** *138*, 259-275.

31. Konishcheva, E. V.; Daubian, D.; Rigo, S.; Meier, W. P., Probing membrane asymmetry of ABC polymersomes. *Chem. Commun.* **2019**, *55*, 1148-1151.

32. Nallani, M.; Andreasson-Ochsner, M.; Tan, C. W.; Sinner, E. K.; Wisantoso, Y.; Geifman-Shochat, S.; Hunziker, W., Proteopolymersomes: in vitro production of a membrane protein in polymersome membranes. *Biointerphases* **2011,** *6* (4), 153-157.

33. Palivan, C. G.; Fischer-Onaca, O.; Delcea, M.; Itel, F.; Meier, W., Protein-polymer nanoreactors for medical applications. *Chem. Soc. Rev.* **2012,** *41* (7), 2800-2823.

34. Sanborn, J. R.; Chen, X.; Yao, Y.-C.; Hammons, J. A.; Tunuguntla, R. H.; Zhang, Y.; Newcomb, C. C.; Soltis, J. A.; De Yoreo, J. J.; Van Buuren, A.; Parikh, A. N.; Noy, A., Carbon Nanotube Porins in Amphiphilic Block Copolymers as Fully Synthetic Mimics of Biological Membranes. *Adv. Mater.* **2018,** *30* (51), 1803355.

35. Messager, L.; Burns, J. R.; Kim, J.; Cecchin, D.; Hindley, J.; Pyne, A. L.; Gaitzsch, J.; Battaglia, G.; Howorka, S., Biomimetic hybrid nanocontainers with selective permeability. *Angew. Chem. Int. Ed.* **2016,** *55* (37), 11106-11109.

36. Schatz, C.; Louguet, S.; Le Meins, J.-F.; Lecommandoux, S., Polysaccharide-block-polypeptide Copolymer Vesicles: Towards Synthetic Viral Capsids. *Angew. Chem. Int. Ed.* **2009,** *48* (14), 2572-2575.

37. Abdelmohsen, L. K.; Nijemeisland, M.; Pawar, G. M.; Janssen, G. J.; Nolte, R. J.; van Hest, J. C.; Wilson, D. A., Dynamic Loading and Unloading of Proteins in Polymeric Stomatocytes: Formation of an Enzyme-Loaded Supramolecular Nanomotor. *ACS Nano* **2016,** *10* (2), 2652-2660.

38. Tu, Y.; Peng, F.; Sui, X.; Men, Y.; White, P. B.; van Hest, J. C. M.; Wilson, D. A., Self-propelled supramolecular nanomotors with temperature-responsive speed regulation. *Nat.Chem.* **2017,** *9* (5), 480-486.

39. Han, G.; Wang, J.-T.; Ji, X.; Liu, L.; Zhao, H., Nanoscale Proteinosomes Fabricated by Self-Assembly of a Supramolecular Protein–Polymer Conjugate. *Bioconjug. Chem.* **2017,** *28* (2), 636-641.

40. Huang, X.; Li, M.; Green, D. C.; Williams, D. S.; Patil, A. J.; Mann, S., Interfacial assembly of protein-polymer nano-conjugates into stimulus-responsive biomimetic protocells. *Nat. Commun.* **2013,** *4*, 2239.

41. Huang, X.; Li, M.; Mann, S., Membrane-mediated cascade reactions by enzyme-polymer proteinosomes. *Chem. Commun.* **2014,** *50* (47), 6278-6280.

42. Gumz, H.; Boye, S.; Iyisan, B.; Krönert, V.; Formanek, P.; Voit, B.; Lederer, A.; Appelhans, D., Toward Functional Synthetic Cells: In-Depth Study of Nanoparticle and Enzyme Diffusion through a Cross-Linked Polymersome Membrane. *Adv. Sci.* **2019,** *6* (7), 1801299.

43. Iyisan, B.; Siedel, A. C.; Gumz, H.; Yassin, M.; Kluge, J.; Gaitzsch, J.; Formanek, P.; Moreno, S.; Voit, B.; Appelhans, D., Dynamic Docking and Undocking Processes Addressing Selectively the Outside and Inside of Polymersomes. *Macromol. Rapid Commun.* **2017,** *38* (21), 1700486.

44. Poschenrieder, S. T.; Klermund, L.; Langer, B.; Castiglione, K., Determination of permeability coefficients of polymersomal membranes for hydrophilic molecules. *Langmuir* **2017,** *33* (24), 6011-6020.

45. Li, M.; Huang, X.; Tang, T. Y.; Mann, S., Synthetic cellularity based on non-lipid micro-compartments and protocell models. *Curr. Opin. Chem. Biol.* **2014,** *22*, 1-11.

46. Liu, X.; Zhou, P.; Huang, Y.; Li, M.; Huang, X.; Mann, S., Hierarchical Proteinosomes for Programmed Release of Multiple Components. *Angew. Chem. Int. Ed.* **2016,** *55* (25), 7095-7100.

47. Marguet, M.; Bonduelle, C.; Lecommandoux, S., Multicompartmentalized polymeric systems: towards biomimetic cellular structure and function. *Chem. Soc. Rev.* **2013,** *42* (2), 512-29.

48. Peters, R. J. R. W.; Marguet, M.; Marais, S.; Fraaije, M. W.; van Hest, J. C. M.; Lecommandoux, S., Cascade Reactions in Multicompartmentalized Polymersomes. *Angew. Chem. Int. Ed.* **2014,** *53* (1), 146-150.

49. Liu, X.; Formanek, P.; Voit, B.; Appelhans, D., Functional Cellular Mimics for the Spatiotemporal Control of Multiple

Enzymatic Cascade Reactions. *Angew. Chem.* **2017,** *129* (51), 16451-16456.

50. Liu, X.; Appelhans, D.; Voit, B., Hollow Capsules with Multiresponsive Valves for Controlled Enzymatic Reactions. *J. Am. Chem. Soc.* **2018,** *140* (47), 16106-16114.

51. Thamboo, S.; Najer, A.; Belluati, A.; von Planta, C.; Wu, D.; Craciun, I.; Meier, W.; Palivan, C. G., Mimicking Cellular Signaling Pathways within Synthetic Multicompartment Vesicles with Triggered Enzyme Activity and Induced Ion Channel Recruitment. *Adv. Funct. Mater.* **2019,** *29* (40), 1904267.

52. Mason, A. F.; Yewdall, N. A.; Welzen, P. L. W.; Shao, J.; van Stevendaal, M.; van Hest, J. C. M.; Williams, D. S.; Abdelmohsen, L. K. E. A., Mimicking Cellular Compartmentalization in a Hierarchical Protocell through Spontaneous Spatial Organization. *ACS Cent. Sci.* **2019,** *5* (8), 1360-1365.

53. Zhao, C.; Zhu, M.; Fang, Y.; Liu, X.; Wang, L.; Chen, D.; Huang, X., Engineering proteinosomes with renewable predatory behaviour towards living organisms. *Mater. Horiz.* **2020,** *7* (1), 157-163.

54. Gobbo, P.; Patil, A. J.; Li, M.; Harniman, R.; Briscoe, W. H.; Mann, S., Programmed assembly of synthetic protocells into thermoresponsive prototissues. *Nat. Mater.* **2018,** *17* (12), 1145-1153.

55. Carlsen, A.; Glaser, N.; Le Meins, J.-F.; Lecommandoux, S., Block Copolymer Vesicle Permeability Measured by Osmotic Swelling and Shrinking. *Langmuir* **2011,** *27* (8), 4884-4890.

56. Choucair, A.; Lim Soo, P.; Eisenberg, A., Active Loading and Tunable Release of Doxorubicin from Block Copolymer Vesicles. *Langmuir* **2005,** *21* (20), 9308-9313.

57. Quan, L.; Ding, H.; Pan, C.; Wei, Y.; Xie, Z., Revealing membrane permeability of polymersomes through fluorescence enhancement. *Colloids Surf. B: Biointerfaces* **2018,** *161*, 156-161.

58. Varlas, S.; Foster, J. C.; Georgiou, P. G.; Keogh, R.; Husband, J. T.; Williams, D. S.; O'Reilly, R. K., Tuning the membrane permeability of polymersome nanoreactors developed by aqueous emulsion polymerization-induced self-assembly. *Nanoscale* **2019,** *11* (26), 12643-12654.

59. Gaitzsch, J.; Appelhans, D.; Wang, L.; Battaglia, G.; Voit, B., Synthetic Bio-nanoreactor: Mechanical and Chemical Control of Polymersome Membrane Permeability. *Angew. Chem. Int. Ed.* **2012,** *51* (18), 4448-4451.

60. Gräfe, D.; Gaitzsch, J.; Appelhans, D.; Voit, B., Cross-linked polymersomes as nanoreactors for controlled and stabilized single and cascade enzymatic reactions. *Nanoscale* **2014,** *6* (18), 10752-10761.

61. Fingernagel, J.; Boye, S.; Kietz, A.; Hobel, S.; Wozniak, K.; Moreno, S.; Janke, A.; Lederer, A.; Aigner, A.; Temme, A.; Voit, B.; Appelhans, D., Mono- and Polyassociation Processes of Pentavalent Biotinylated PEI Glycopolymers for the Fabrication of Biohybrid Structures with Targeting Properties. *Biomacromolecules* **2019,** *20* (9), 3408-3424.

62. Daeg, J.; Xu, X.; Zhao, L.; Boye, S.; Janke, A.; Temme, A.; Zhao, J.; Lederer, A.; Voit, B.; Shi, X.; Appelhans, D., Bivalent Peptide- and Chelator-Containing Bioconjugates as Toolbox Components for Personalized Nanomedicine. *Biomacromolecules* **2020,** *21* (1), 199-213.

63. Gaitzsch, J.; Appelhans, D.; Grafe, D.; Schwille, P.; Voit, B., Photo-crosslinked and pH sensitive polymersomes for triggering the loading and release of cargo. *Chem. Commun.* **2011,** *47* (12), 3466-8.

64. Iyisan, B.; Kluge, J. r.; Formanek, P.; Voit, B.; Appelhans, D., Multifunctional and dual-responsive polymersomes as robust nanocontainers: design, formation by sequential post-

conjugations, and pH-controlled drug release. *Chem. Mater.* **2016,** *28* (5), 1513-1525.

65. Gumz, H.; Lai, T. H.; Voit, B.; Appelhans, D., Fine-tuning the pH response of polymersomes for mimicking and controlling the cell membrane functionality. *Polym. Chem.* **2017,** *8* (19), 2904-2908.

66. Moreno, S.; Sharan, P.; Engelke, J.; Gumz, H.; Boye, S.; Oertel, U.; Wang, P.; Banerjee, S.; Klajn, R.; Voit, B.; Lederer, A.; Appelhans, D., Light-Driven Proton Transfer for Cyclic and Temporal Switching of Enzymatic Nanoreactors. *Small* **2020,** https://doi.org/10.1002/smll.202002135

67. Yao, Z.; Zhang, M.; Sakahara, H.; Saga, T.; Arano, Y.; Konishi, J., Avidin targeting of intraperitoneal tumor xenografts. *J. Natl. Cancer Inst.* **1998,** *90* (1), 25-29.

68. Rosano, C.; Arosio, P.; Bolognesi, M., The X-ray three-dimensional structure of avidin. *Biomol. Eng.* **1999,** *16* (1-4), 5-12.

69. Livnah, O.; Bayer, E. A.; Wilchek, M.; Sussman, J. L., Three-dimensional structures of avidin and the avidin-biotin complex. *Proc Natl Acad Sci U S A* **1993,** *90* (11), 5076-5080.

70. Jain, A.; Cheng, K., The principles and applications of avidin-based nanoparticles in drug delivery and diagnosis. *J. Controlled Release* **2017,** *245*, 27-40.

71. Batchelor, R.; Sarkez, A.; Gregory Cox, W.; Johnson, I., Fluorometric Assay for Quatification of Biotin Covalently Attached to Proteins and Nucleic Acids. *Biotechniques*, 2007, **43**, 503-507.

72. Ccorahua, R.; Moreno, S.; Gumz, H.; Sahre, K.; Voit, B.; Appelhans, D., Reconstitution properties of biologically active polymersomes after cryogenic freezing and a freeze-drying process. *RSC Adv.* **2018,** *8* (45), 25436-25443.

73. Cheng, R.; Meng, F.; Ma, S.; Xu, H.; Liu, H.; Jing, X.; Zhong, Z., Reduction and temperature dual-responsive crosslinked polymersomes for targeted intracellular protein delivery. *J. Mater. Chem.* **2011,** *21* (47), 19013-19020.

74. Meng, F.; Zhong, Z.; Feijen, J., Stimuli-Responsive Polymersomes for Programmed Drug Delivery. *Biomacromolecules* **2009,** *10* (2), 197-209.

75. Garni, M.; Thamboo, S.; Schoenenberger, C. A.; Palivan, C. G., Biopores/membrane proteins in synthetic polymer membranes. *Biochim. Biophys. Acta. Biomembranes* **2017,** 1859 (4), 619-638

Supporting Information

Avidin locations in pH-responsive polymersomes for probing the docking of biotinylated (macro)molecules in the membrane and lumen

Silvia Moreno[a]*, Susanne Boye[a], Albena Lederer[a,b], Annarita Falanga[c], Stefania Galdiero[d], Sébastien Lecommandoux[e], Brigitte Voit[a,b], Dietmar Appelhans[a]*

[a] Leibniz-Institut für Polymerforschung Dresden e.V., Hohe Straße 6, 01069 Dresden, Germany

[b] Organic Chemistry of Polymers, Technische Universität Dresden, 01062 Dresden, Germany

[c] Department of Agricultural Science, University of Naples "Federico II", Via dell'Università 100, 80055, Portici, Naples, Italy

[d] Department of Pharmacy, University of Naples "Federico II", Via Mezzocannone 16, 80134 Naples, Italy; CiRPEB, University of Naples "Federico II", Via Mezzocannone 16, 80134 Naples, Italy

[e] Univ. Bordeaux, CNRS, Bordeaux INP, LCPO, UMR 5629, F-33600, Pessac, France

*Corresponding author: applhans@ipfdd.de and moreno@ipfdd.de

Content of SI   Page

1. Materials

Poly(ethylene glycol) methyl ether (MeO-PEG-OH; M_n = 2000 g/mol^{-1}; M_w/M_n = 1.05), 2,2´-bipyridine, 4-aminobutanol, diethylaminoethyl methacrylate (DEAEM), methacryloylic chloride, 2-bromoisobutyryl bromide, 2-aminoethanol, copper-I-bromide, aluminum oxide (neutral, activated), phosphate buffered saline (tablet), fluorescein-5(6)-isothiocyanat (FITC), sodium hydroxide, dimethyl sulfoxide (DMSO) and albumin from human serum (HSA) were purchased from Sigma-Aldrich. 3,4-Dimethylmaleic acid anhydride, toluene, THF, ethyl acetate and chloroform-d were purchased from Acros Organics. *n*-Hexane, hydrochloric acid (37%) and silica gel were purchased from Merck (Germany). Avidin, Egg White, Avidin.Alexa488 conjugate, biotinylated horseradish peroxidase (bHRP) and 4-hydroxyazobenzene-2-carboxylic acid (HABA) were purchased from ThermoFisher Scientific. Biotin-DOOA*HCl, Biotin-PEG-NH$_2$ (M_n = 3 kDa), Biotin-PEG-NH$_2$ (M_n = 5 kDa) and Biotin-PEG-NH$_2$ (M_n = 10 kDa) were purchased from Iris Biotech GmbH (Germany). Biotinylated glucose oxidase was purchased from Biomol (Germany). bTAT (peptide cell penetrated, H-GRKKRRQRRRPQK(Biotin)-NH$_2$) was purchased from Pepscan (Netherlands). Catalase, biotin labeled, was purchased from Nanocs (Germany). Anhydrous 2-butanone (Fluka), triethylamine (Fluka) and anhydrous tetrahydrofuran (THF, Sigma-Aldrich) were stored over a molecular sieve. bCPP, bPPI, bHA, bHSA and bPNIPAm were synthesized and characterized by our working groups (more information in the Section 4).

2. Devices

NMR Spectroscopy. Bruker Advance III 500 spectrometer (Bruker Biospin, Germany) was used for recording ^{1}H NMR (500.13 MHz) spectra using CDCl$_3$ or D$_2$O as solvent at room temperature. The chemical shifts were referenced to corresponding solvent signals (CDCl$_3$: δ = 7.26 ppm; D$_2$O: δ = 4.60 ppm) and were expressed in ppm.

Gel Permeation Chromatography. The molar mass distributions (Đ), weight average molecular weight (M_w), number average molecular weight (M_n) of block copolymers were measured using SEC equipped with a MALLS detector (MiniDAWN-LS detector, Wyatt Technology, USA) and a viscosity/refractive index (RI) detector (ETA-2020, WGE Dr. Bures, Germany). The column (PL MIXED-C with a pore size of 5 μm, 300x7.5 mm) and the pump (HPLC pump, Agilent 1200 series) were from Agilent Technologies (USA). THF was used as an eluent (stabilized with 0.025 % BHT) with a flow rate of 1 mL/min. The calibration was performed on polystyrene standards ranging from 1300 to 377400 g/mol.

Hollow Fiber Filtration. This filtration technique is used to remove the unbounded moieties which could not get encapsulated in the polymersomes during the self-assembly process. HFF was carried out using KrosFlo Research Iii System. This device was equipped with a separation module made of polyether sulfone membrane (MWCO: 500 kDa, SpectrumLabs, USA). The transmembrane pressure was 150 mbar with a flow rate of 15 mL/min.

Dynamic Light Scattering. DLS measurements of aqueous polymersome solutions (≤ 1 mg/mL) were carried out using a Zetasizer Nano-series instrument (Malvern Instruments, UK) equipped with

Dispersion Technology Software (version 5.00). The measurements were carried over a range of pH at 20°C. The data was collected using the NIBS (non-invasive back-scatter) method using a Helium–Neon laser (4 mW, l = 632.8 nm) and a fixed angle of 173°. The data was analyzed using Malvern Software 7.11.

Zeta potential (ζ). ζ measurements were carried out on all used biotinylated compounds (1 mg/mL) at a pH 7.4 and at 25°C using a Zetasizer Nano-series instrument (Malvern Instruments, UK) through electrophoretic light scattering. Data evaluation was carried out by using Malvern Software 7.11.

UV-VIS. Instrument: Cary 6000i (Varian); Spectral band with (SBW): 1 nm; Reference: Millipore; Sample thickness: 4 mm; Integration time: 0.3 s; Detector: Cary 6000i.

Fluorescence intensity. Fluorescence spectra were measured Fluorolog 3 (Horiba JobinYvon, USA) fluorescence spectrophotometer. $C_{sample} = 0.25$ mg/mL Psome; $\lambda_{exc} = 534$ nm.

UV lamp: cross-linking of the block copolymer. EXFO Omnicure 1000 (Lumen Dynamics GroupInc., Canada) equipped with a high pressure mercury lamp as UV source was used for crosslinking the polymersomes (320-500 nm).

Asymmetrical Flow Field-Flow Fractionation (AF4). AF4 measurements were performed with an Eclipse DUALTEC system (Wyatt Technology Europe, Germany) with 0.001 M PBS buffer at pH 8 as carrier liquid and 0.02% (w/v) NaN_3 to prevent growth of bacteria and algae. The channel spacer made of poly(tetrafluoroethylene) had a thickness of 490 µm, and the channel dimensions were 26.5 cm in length and from 2.1 to 0.6 cm in width. The membranes used as accumulation wall were composed of regenerated cellulose with a molecular weight cut off (MWCO) of 10 kDa (Superon GmbH, Germany). Flow rates were controlled with an Agilent Technologies 1260er series isocratic pump equipped with vacuum degasser. The detection system consists of a MALS detector (DAWN HELEOS II, Wyatt Technology Europe, Germany) operating at a wavelength of 660 nm with online DLS detector (DynaProNanoStar, Wyatt Technologies, USA) which is an add-on unit connected to the 99° angle of the MALS, a variable wavelength detector (1260 series, Agilent Technologies Deutschland), a variable wavelength detector (VWD, 1260er series, Agilent Technologies, Germany), and a refractive index (RI) detector (Optilab T-rEX, Wyatt Technology Europe GmbH, Germany) operating at a wavelength of 660 nm. All injections were performed with an autosampler (1260 series, Agilent Technologies Deutschland GmbH). The data collection and calculation of molar masses and radii were performed by Astra 6.1.2.84 software (Wyatt Technologies, USA). The channel flow rate (Fc) was maintained at 1 mL min^{-1} for all AF4 measurements at 25°C. If not mentioned otherwise, the focus flow (F$_f$) was set at 1.5 mL min^{-1} for 8 min. The injection volume was set to 300 µL. Depending on the studied system, different measurement profiles were applied. Polymersome samples were separated by following parameters: the separation starts with an isocratic step with a cross flow rate (F$_x$) of 2 mL min$_{-1}$ for 15 min followed by a linear F$_x$ gradient from 2 to 0 mL min^{-1} within 2 min. The last step proceeds without F$_x$ (0 mL min^{-1}) for 20 min. Recovery tests with varied sample loads verified that no adsorption takes place at fresh membranes.
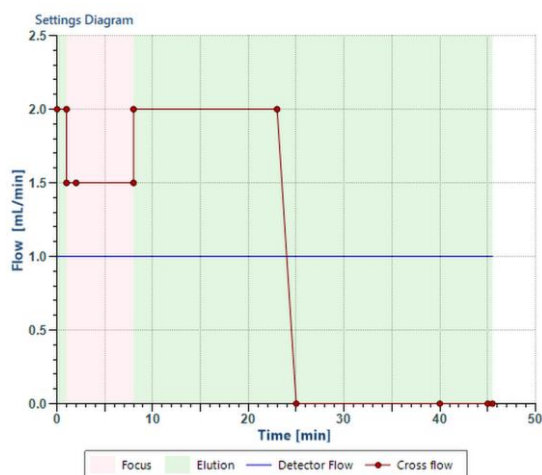
Scaling parameter AF4 study:

By plotting R_g vs M, n can be determined by the slope of the plot, it gives information about the molecular shape in the used solvent

$R_g = K \cdot M^n$

$v = 0.33$ (sphere)

$v = 0.5 – 0.6$ (random coil macromolecule)

$v = 1$ (rigid rod)

Apparent density for AF study:

Give information about molecular density, is calculated by R_g and M_w (with V as volume fraction, a as geometrical correction, N_A as Avodgadro's number):

$$d_{app,i} = \frac{M_i}{V(R_g)_i \cdot N_A} \cdot \alpha \quad \text{with} \quad \alpha = \frac{V_{sphere}(R_g)}{V_{sphere}(R)} = \frac{R_g{}^3}{R^3} = \frac{\left(\sqrt{\frac{3}{5}} \cdot R\right)^3}{R^3} = \left(\frac{3}{5}\right)^{\frac{3}{2}}$$

ρ Parameter:

The ratio between R_g and R_h delivers valuable information about conformation and shape of molecules, some examples[1]:

Homogeneous sphere: 0.775

Random coil, linear chain (good solvent):   1.78

Hyperbranched polymer: 1.23

Rod (axial ratio = 2.5):   2.1

Cryo-TEM. Cryo-TEM images were acquired using Libra 120 microscope (Carl Zeiss Microscopy GmbH, Oberkochen, Germany) at an acceleration voltage of 120 kV. Samples were prepared by

5

dropping 2 µL of polymersome solution (1 mg mL^{-1}) on copper grids coated with holey carbon foil (so-called Lacey type). The excess of the solution was removed by filter paper; the sample was then rapidly frozen in liquid ethane at -178 °C. The blotting with the filter paper and plunging into liquid ethane was done in a Leica GP device (Leica Microsystems GmbH, Wetzlar, Germany). All images were recorded in bright field at -172 °C. The diameter and membrane thickness of the polymersome were determined from cryo-TEM images by using iTEM image processing software by Olympus (Olympus Soft Imaging Solutions GmbH, Münster, Germany). Several polymersome particles were analyzed at pH 8 state. The polymersome diameter was measured from images taken at more than 6000x magnification, while the membrane thickness was measured from images taken at 16 000x magnification ahead. The average was calculated by analyzing 250 particles for each sample.

FTIR. It was performed using FTIR-Spektrometer Vertex 80v (Bruker). Golden Gate Diamond ATR unit (SPECAC). MCT-Detector. 4000–600 cm^{-1}. Resolution = 4 cm^{-1}, 100 scans per measurement.

Matrix-assisted laser desorption/ionization time of flight mass spectrometry (MALDI-TOF MS): MALDI-TOF MS was performed using Autoflex Speed TOF/TOF System (Bruker Daltonics GmbH). The measurements were carried out in a linear mode and positive polarity by pulsed smart beam laser (modified Nd:YAG laser). The ion acceleration voltage was set to 20 kV. For the sample preparation, the polymers were mixed with sinapinic acid as matrix both dissolved in a mixture of acetonitrile and 1% aqueous formic acid in a ratio of 1:1 by volume. The preparation was done without salt.

Raman. It was performed using RAMAN Imaging System WITEC alpha300R. Laser: 532 nm. Laser power: 5 mW (PraCPP) / 2 mW (biotinCPP). Objective: 20x. Integration time: 0.5 s. Accumulations: 500. Spectral resolution: 3 cm-1 (+/- 1.5 cm^{-1}).

Microplate reader. TECAN infinite PRO microplate reader equipped with I-control 1.10 software was used for studying FRET experiment. Measurements were carried out at a wavelength λ = 317 nm and 488 nm and bandwidth of 9 nm at 37°C.

3.   Synthesis and characterization of block copolymer

The block copolymer (BCP) was synthesized by using standard ATRP procedure as reported previously.[2-5] PEG$_{45}$-Br (100 mg), 3,4-dimethylmaleinimidobutylmethacrylate (246.9 mg, 20 eq), diethylaminoethylmethacrylate (603.4 mg, 70 eq), bipyridine (14.5 mg, 2 eq) were mixed together with ethylmethylketone (1.5 mL). Under the nitrogen atmosphere, Cu(I)Br (6.7 mg, 1 eq) was added to the mixture. This mixture was deoxygenated by freeze pump thaw cycles. Finally, the mixture was then refluxed for 19 hours at 50°C. Later, the polymerization was terminated by exposure of the mixture to air by adding THF. The oxidized copper catalyst was removed by passing through the mixture over an activated neutral aluminium oxide with THF as an eluent, and the solution was filtered using 0.2 µm filter. Final solution was concentrated by evaporating most of the solvent, followed precipitation in cold n-hexane. Later, a dialysis was carried out in acetone in a membrane of size 2000 kDa for 24 h. The composition of **BCP** was determined by ^{1}H-NMR and SEC-MALLS. The composition and the number average molecular weight (M$_n$) of **BCP** were determined with ^{1}H NMR spectroscopy from the peak

integrals of PEG (3.65 ppm), DEAEMA (2.65-2.78 ppm) and DMIBM (3.52 ppm) by taking the PEG block as an internal standard. Additionally, the molar mass distributions (Đ) were determined by SEC as described in previous section. **Table S1** shows the corresponding results.

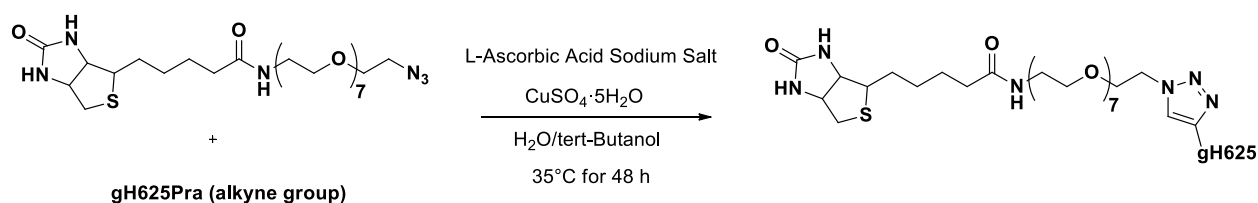## 4. Synthesis and characterization of biotinylated compounds
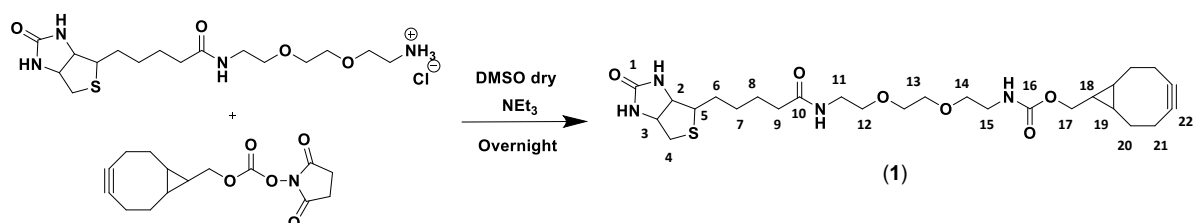
bPEGCOD500 (~500 g/mol (1)): To a solution of Biotin-DOOA*HCl (50 mg, 0.133 mmol) (CAS-NO 862373-14-6) in DMSO dry was added NEt₃ (37.2 µL, 0.267 mmol) and (1R,8S,9s)-bicyclo[6.1.0]non-4-yn-9-ylmethyl N-succinimidyl carbonate (COD) (42.8 mg, 0.147 mmol). After 2 days of stirring at room temperature, the crude product was dissolved in a mixture DCM/H_2O (1:1), the combined organic phases were dried with $MgSO_4$, and the solvent was removed in vacuum. Checking the ^{1}H-NMR, if it is not pure, the residue is additionally purified by column chromatography in THF (55 mg, Yield 75 %). ^{1}H-NMR (500 MHz, DMSO-d_6, δ): 0.86 (t, H_{19}, 2H), 1.20-1.40 (m, H_{18}, 1H, H_7, 2H), 1.40-1.65 (m, H_{20}, 4H; H_6 and H_8, 4H), 2.06 (t, H_9, 2H), 2.10-2.32 (m, H_{21}, 4H), 2.58 (dd, H_{4A}, 1H), 2.82 (dd, H_{4B}, 1H), 3.11 (m, H_5, 1H), 3.18 (m, H_{11}, 2H), 3.30 (m, overlapped with H_2O, H_{15}, 2H), 3.39 (s, H_{12}, H_{13}, H_{14}, 8H), 4.03 (d, H_{17}, 2H), 4.13 (m, H_3, 1H), 4.30 (m, H_2, 1H), 6.32 (s, NHCONH, 1H), 6.38 (s, NHCONH, 1H), 7.04 (s, NHCO, 1H), 7.79 (s, NHCO, 1H). ^{13}C {^{1}H}-NMR (500 MHz, DMSO-d_6, δ): 18.1 (C_{18}), 20.1 (C_{19}), 21.3 (C_{21}), 25.7 (C_8), 28.6(C_6), 29.0 (C_7), 29.2 (C_{20}), 35.6 (C_9), 38.9 (C_{11}), 40.0 (C_4, C_{15}, DMSO overlapped), 55.9 (C_5), 59.6 (C_3), 61.5 (C_2), 61.9 (C_{17}), 69.5 (C_{12}, C_{14}), 69.9 (C_{PEG}), 99.5 (C_{22}), 163.1 (C_1), 172.6 (C_{10}). **Figure S11** shows the corresponding ^{1}H-NMR. M_w= 550.72 g/mol
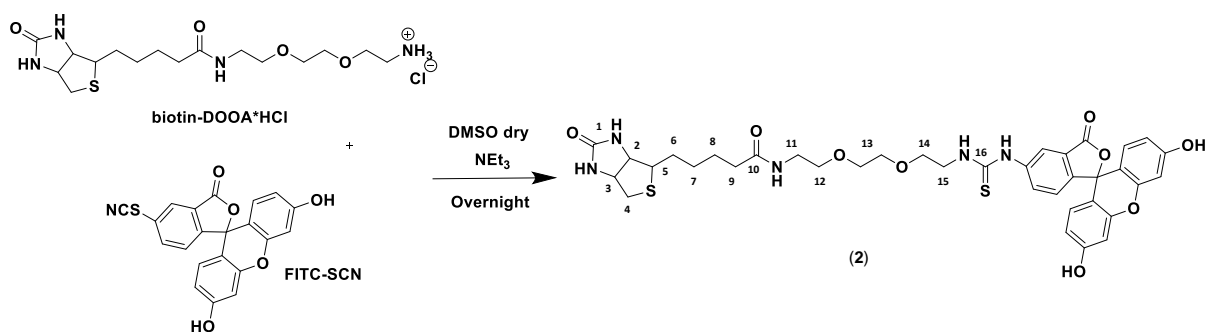
bPEGFITC500 (2): To a solution of Biotin-DOOA*HCl (20 mg, 0.049 mmol) (CAS-NO 862373-14-6) in DMSO dry was added NEt₃ (13.6 µL, 0.097 mmol) and stirred for 2 hours before adding FITC-SCN (21 mg, 0.053 mmol) solution in DMSO (0.5 mL). After 20 hours of stirring at room temperature,

the mixture was the product was purified by chromatography of exclusion steric in THF (25 mg, Yield 68%). ^{1}H-NMR (500 MHz, DMSO-d$_6$, δ): 1.20-1.65 (m, H$_6$, H$_7$, and H$_8$, 6H), 2.06 (t, H$_9$, 2H), 2.57 (dd, H$_{4A}$, 1H), 2.81 (dd, H$_{4B}$, 1H), 3.08 (m, H$_5$, 1H), 3.18 (m, H$_{11}$, 2H), 3.30 (m, overlapped with H$_2$O, H$_{15}$, 2H), 3.38-3.80 (m, H$_{12}$, H$_{13}$, H$_{14}$, H$_{15}$, 10H), 4.12 (m, H$_3$, 1H), 4.29 (m, H$_2$, 1H), 6.34 (s, N*H*CONH, 1H), 6.38 (s, NHCON*H*, 1H), 6.50-8.35 (FITC), 7.80 (s, N*H*CO, 1H), 8.08 (s, N*H*CS, 1H), 10.05 (s, N*H*CS, 1H). ^{13}C {^{1}H}-NMR (500 MHz, DMSO-d$_6$, δ): 18.1 (C$_{18}$), 19.6 (C$_{19}$), 20.9 (C$_{21}$), 25.3 (C$_8$), 28.1(C$_6$), 28.2 (C$_7$), 28.6 (C$_{20}$), 35.1 (C$_9$), 38.5 (C$_{11}$), 40 (C$_4$, C$_{15}$, DMSO overlapped), 55.4 (C$_5$), 59.2 (C$_3$), 61.1 (C$_2$), 61.4 (C$_{17}$), 69.2 (C$_{12}$, C$_{14}$), 69.8 (C$_{PEG}$), 99.0 (C$_{22}$), 162.7 (C$_1$), 172.2 (C$_{10}$), 180.1 (C=S, C$_{16}$). **Figure S12** shows the corresponding ^{1}H-NMR. M$_w$= 763.88 g/mol

gH625Pra (alkyne group)

L-Ascorbic Acid Sodium Salt
CuSO$_4$·5H$_2$O
H$_2$O/tert-Butanol
35°C for 48 h

gH625

CPP (gH625Pra, 2391.3 g/mol): The peptide gH625Pra (NH$_2$-HGLASTLTRWAHYNALIRAF-Pra-CONH$_2$) was synthesized as previously reported[6] by the standard solid-phase 9-fluorenylmethoxycarbonyl (Fmoc) method by using a Syro I MultiSynThec GmbH (Wullener, Germany) automatic synthesizer. The Rink amide MBHA resin (substitution 0.51 mmol g^{-1}) was used as the solid-phase support, and syntheses were performed on a scale of 20 mmol. Fmoc-protected amino acids (4 equiv relative to resin loading), were coupled according to the PyBop/HOBt/DIPEA method: Fmoc-amino acid (1 equiv), PyBOP (1 equiv), HOBt (0.5 mm in DMF, 1 equiv), and DIPEA (1.0 mm in DMF, 2 equiv). The Fmoc protecting group was removed with 30% piperidine in DMF (v/v). All couplings were performed twice for 1 h. Fmoc-Pra-OH was coupled once for 45 min with 2 equivalents of PyBop/HOBt and 2 equivalents of DIPEA. Peptides were fully deprotected and cleaved from the resin with TFA with 2.5% (v/v) water, 2.0% (v/v) anisole, and 2.0% (v/v) thioanisole as scavengers, at room temperature, and then precipitated with ice-cold ethyl ether, filtered, dissolved in water, and lyophilized. The crude peptide was purified by RP-HPLC on a LC8 Shimadzu HPLC system (Shimadzu Corporation,Kyoto, Japan) equipped with a UV lambda-Max Model 481 detector using a Phenomenex (Torrance, CA) C18 (300 Å, 250 x 21.20 mm, 5 m) column eluted with H$_2$O/0.1% TFA (A) and CH$_3$CN/0.1% TFA (B) from 20–80% over 20 min at a flow rate of 20 mL min^{-1}. Purity and identity were assessed by analytical LC-MS analyses by using Finnigan Surveyor MSQ single quadrupole electrospray ionization (Finnigan/Thermo Electron Corporation San Jose, CA), column: C18-Phenomenex eluted with H$_2$O/0.1% TFA (A) and CH$_3$CN/0.1% TFA (B) from 20–80% over 10 min at a flow rate of 0.8 mL min^{-1}. The final yields of purified peptides ranged between 20 and 40%.

bCPP (3000 g/mol) – b6 (3) : 4.1 mg of CPP (1 Eq, M$_w$ = 2391.55 g/mol, 0.0017 mmol of CPP (gH625Pra), 1.6 mg of biotin-dPEG-N$_3$ (1.5 Eq, M$_w$ = 620.76 g/mol, 0.0026 mmol) and 0.4 mg L-Ascorbic Acid Sodium Salt (1.4 Eq, M$_w$ = 176.12 g/mol, 0.0024 mmol) were added into 4 ml H$_2$O and

1 ml *tert*-Butanol. 0.43 mg $CuSO_4*5H_2O$ (1 Eq, M_w = 249.67 g/mol, 0.0017 mmol) was added after 20 min under Ar. Then the mixture was stirred at 35°C for 48 h. The reaction mixture was purified by dialyzing in deionized water for 48 h, including repeating exchanges of deionized water. After removal of the water by freeze drying, wheat white solid was obtained (3.5 mg, yield: 69 %). **Figure S15** shows the corresponding Raman spectrum.
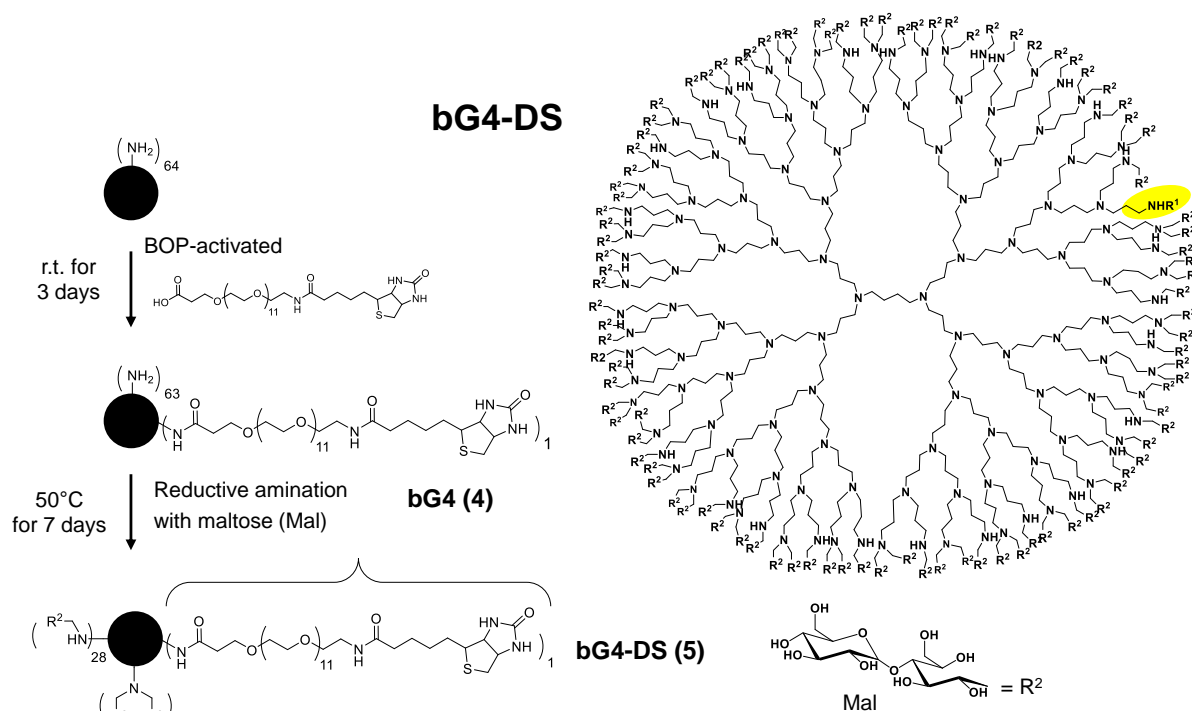

bG4-DS – b7 (4-5): Synthesis of Biotin-PEG$_{12}$-modified 4th generation poly(propyleneimine) (PPI) dendrimer (bG4) – 30 ml DMSO was dried and degassed for around 1 h under high vacuum. 4th generation poly(propylenimine), DAB-Am-64 (PPI; M_w = 7162.96 g/mol; 1 equivalent; 503 mg; 7.02×10^{-5} mol) was dissolved in 2/3 of vacuum-treated DMSO before adding triethylamine (0.5 ml). Alpha-biotin-omega-(propionic acid)-dodecae(ethylene glycol) (PEG12-B; M_w 844.04 g/mol; 1 equivalent; 59 mg; 7.02×10^{-5} mol) and (benzotriazol-1-yloxy)tris(dimethylamino)phosphonium hexafluorophosphat (BOP; M_w 442.28 g/mol; 1.5 equivalent; 46 mg; 1.05×10^{-4} mol) were dissolved in 1/3 of vacuum-treated DMSO. The resulting reaction mixture was stirred for 1 h at room temperature under argon atmosphere. PPI solution was added to the ester-active PEG12-B solution. This reaction mixture was stirred for 3 days at room temperature under argon atmosphere and was then dialyzed for 3 days in water (MWCO: 1000; exchanging water several times). After freeze drying process of dialyzed product bG4 a viscous liquid was obtained (yield: 97.9 (0.549 mg)). ^1H NMR spectrum of bG4-DS in D_2O is the same for G4-DS-PEG12B1 as published in F. Ennen et al. (Figure 2 + 3):[7] *Synthesis of PEG12-B-modified 4th generation poly(propyleneimine) glycodendrimer (bG4-DS)* - bG4

9

(M_{theo} = 7989 g/mol; 1 equivalent; 76 mg; 9.51x10⁻⁶ mol) was stirred in sodium-borate buffer (0.1 M) for one hour at 50°C. After that sugar (maltose monohydrate; M_w 360.31 g/mol; 1270 equivalents; 4.35 g; 1.21×10^{-2} mol) was added to the solution and the reaction mixture was additionally stirred for one hour at 50°C. Borane*pyridine complex ($BH_3 \times$ Pyr - 8 M; 1270 equivalents; 1.51 ml; 1.21×10^{-2} mol) was lastly added, then the reaction mixture was stirred for 7 days at 50°C under reflux. Then the desired crude product was dialyzed for 4 days in water (MWCO: 2000 g/mol; extensive exchange of double-distilled water) and after freeze drying a white solid was obtained (yield: 92% (0.427 g)). ¹H NMR spectrum of **bG4-DS** in D_2O is the same for G4-DS-PEG12B1 as published in F. Ennen et al. (Figure 2 + 3):[7]. Molecular weight was determined by MALDI-TOF-MS: 43,200 g/mol. Degree of biotinylation by HABA assay: 0.7.

b9 (**6**)
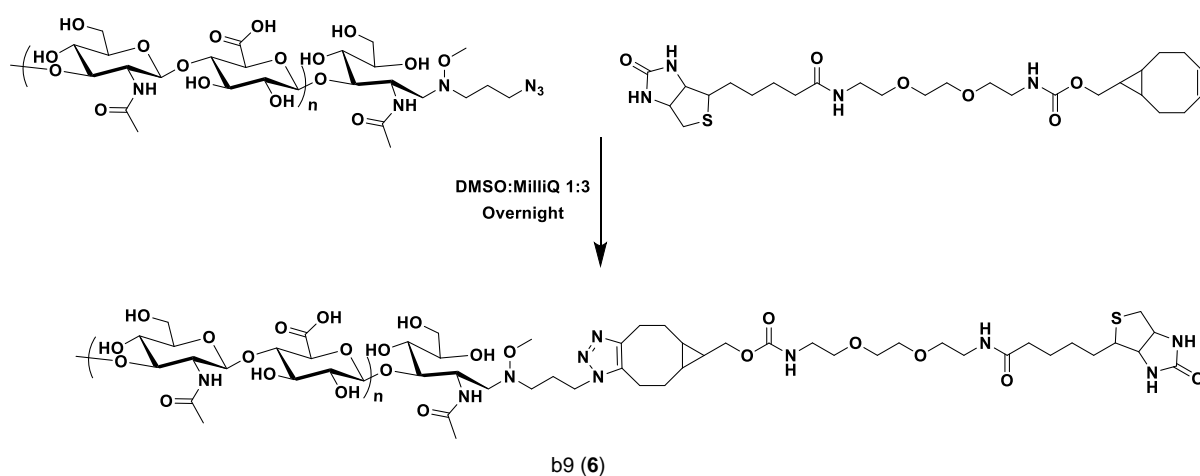
Precursor HA-N₃: The preparation of HA-N3 was performed from a commercially available hyaluronan (Lifecore Biomedical research grade HA-5kDa with a molar mass MW = 7000 g/mol, Đ 1.49) following a previously reported method[8] that consists in coupling propargylamine to the reducing end of hyaluronan, using sodium cyanoborohydride (NaCNBH₃) as a reducing agent in acetate buffer at room temperature.

bHA-b9 (6): To a solution of bPEGCOD₅₀₀ (2.4 mg, 0.0043 mmol) in DMSO/MilliQ water (ratio 1:3) was added HA-N₃ (20 mg, 0.0029 mmol). After 20 hours of stirring at room temperature, the crude product was purified by dialysis using membrane with MWCO 2 kDa (15 mg, Yield 70%). HA-Azide (Đ 1.49, 7000 g/mol). **Figure S13** shows the corresponding ¹H-NMR. **FT-IR** (cm⁻¹): 3292 (O-H, N-H), 2888 (CH), 1602 (C=O), 1025(C-O). Band disappearance 2104 cm-1 (N₃) corroborates the complete modification. **Figure S14** shows the corresponding FT-IR.
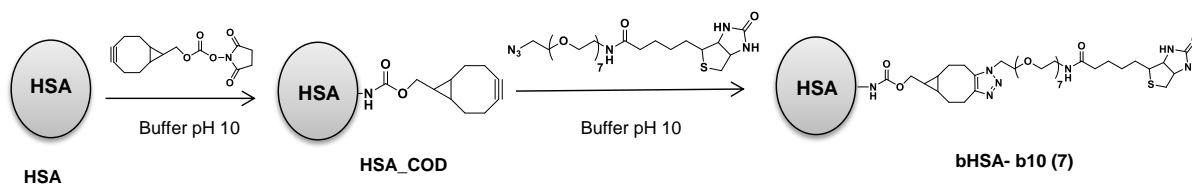
bHSA-b10 (7) *.* Stock solutions are prepared for (1R,8S,9s)-bicyclo[6.1.0]non-4-yn-9-ylmethyl N-succinimidyl carbonate (COD) (2 mg in 200 mL DMSO) and biotin-dPEG(7)-N$_3$ (2 mg in 200 mL DMSO). *HSA-COD.* Albumin from human serum (HSA) (10 mg, 0.15 µmol) was dissolved in 500 mL carbonate buffer (pH 10) and stirred for 30 min before adding COD solution in DMSO (14 µL, 0.47 µmol). After 20 hours of stirring at room temperature, the mixture was extensively dialyzed against 1 mM PBS for 2 days (dialysis membrane: 3.5–5 kDa MWCO) to remove all unbounded molecules. Finally, the purified mixture was freeze dried overnight and the white product was isolated. MALDI-TOF-MS: 67500 g mol^{-1} (3-4 COD groups attached to HSA).[2] *HSA-biotin.* HSA-COD (10 mg, 0.15 µmol) was dissolved in 500 mL in carbonate buffer (pH 10) and stirred for 30 min before biotin-dPEG-N$_3$ (6 Eq, 14 µL, 0.56 mg, 0.9 µmol, M$_w$ = 620.76 g/mol). After 48 hours of stirring at room temperature, the mixture was extensively dialyzed against 1 mM PBS for 2 days (dialysis membrane: 3.5–5 kDa MWCO) to remove all unbounded molecules. Finally, the purified mixture was freeze dried overnight and the white product was isolated.
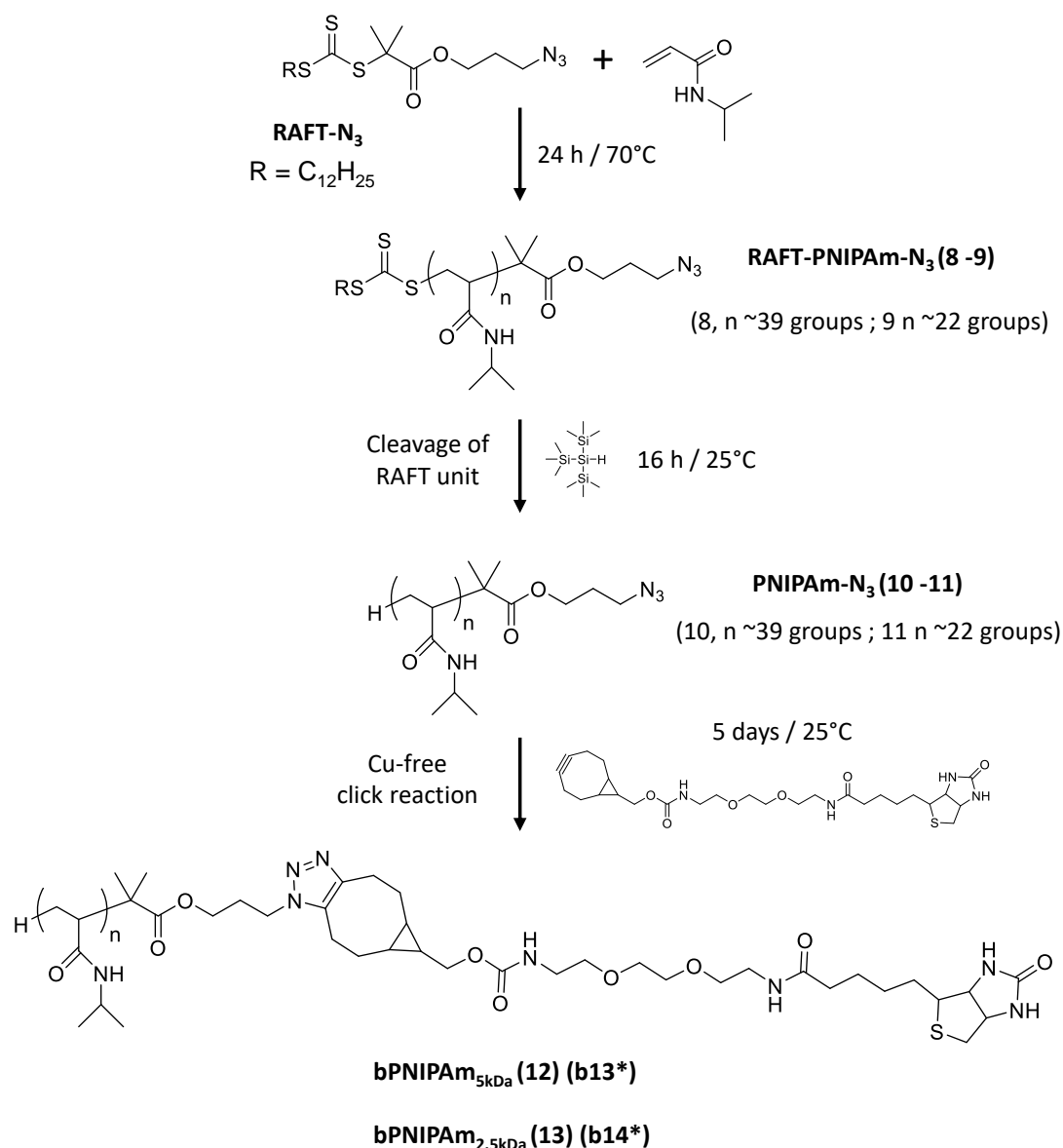
Synthesis of biotinylated poly(N-isopropylacrylaminde) (bPNIPAm)

Synthesis of azido-modified PNIPAm (RAFT-PNIPAm-N3)(8-9) - *N*-Isopropylacrylamide (NIPAm, M_w 113.16 g/mol), azobisisobutyronitrile (AIBN, M_w 164.21 g/mol) and 2-(dodecylthiocarbonothioylthio)-2-methylpropionic acid 3-azido-1-propanol ester (RAFT-N3, M_w 447.72 g/mol) und 1,4-dioxane were collected in a dry Schlenk flask with magnetic stir bare under argon atmosphere. The solution was degassed using at least 4-freeze-pump-thaw cycles. After this process the solution was kept under argon atmosphere and stirred at 70°C for 24h. Subsequently the reaction solution was quenched by liquid nitrogen and the solvent was removed in vacuum through the use of a rotary evaporator. The crude product RAFT-PNIPAm-N3 was purified twice by the precipitation in THF/*n*-hexane. RAFT-PNIPAm-N3 was obtained as a white-yellow solid. Used concentration for the synthesis of RAFT-PNIPAm-N3 with corresponding molecular weights of 2,500 and 5,000 g/mol are presented in **Table S1**. RAFT-PNIPAm-N3 was characterized by ¹H NMR (see **Figure S16** for RAFT-PNIPAm-N3).

Synthesis of PNIPAm-N₃ through the cleavage of RAFT unit (10-11) - RAFT-polymer-N₃ (RAFT-PNIPAm-N₃-A with M_w 5,000 g/mol or RAFT-PNIPAm-N₃-B with M_w 2,500 g/mol), azobisisobutyronitrile (AIBN, M_w 164.21 g/mol), tris(trimethylsilyl)silane (TTMSS, M_w 248.66 g/mol) and 1,4-dioxane were collected in a dry Schlenk flask with magnetic stir bare under argon atmosphere. The solution was degassed using at least 4-freeze-pump-thaw cycles. After this process the solution was kept under argon atmosphere and stirred at 40°C for 16h. Subsequently the reaction solution was quenched by liquid nitrogen and the solvent was removed in vacuum through the use of a rotary evaporator. The crude product PNIPAm-N₃ was purified twice by the precipitation in THF/*n*-hexane. Then the crude product PNIPAm-N₃ was dialyzed (MWCO: 1000 g/mol) for 2 days against water/THF (1:3) and THF was distilled off by the use of rotary evaporator. The residual solution was finally freeze-dried. PNIPAm-N₃ was obtained as white solid. Used concentration for the synthesis of PNIPAm-N₃ with corresponding molecular weights of 2,500 and 5,000 g/mol are presented in **Table S2**. PNIPAm-N₃ was characterized by ¹H NMR (see **Figure S17** for PNIPAm-N₃).

Biotinylation of PNIPAm-N₃ (bPNIPAm) (12-13) - PNIPAm-N₃ (PNIPAm-N₃-A with M_w 5,000 g/mol or RAFT-PNIPAm-N₃-B with M_w 2,500 g/mol) und bPEGCOD₅₀₀ (M_w 550.72 g/mol) were dissolved in mixture of H₂O/THF (1:3). The reaction solution was stirred at 25°C for 5 days under light protection and argon atmosphere. Finally, the reaction mixture was dialyzed (MWCO: 1000 g/mol) for three days against water/THF (1:3) and THF was distilled off by the use of rotary evaporator. The residual solution was finally freeze-dried. bPNIPAm was obtained as white solid. Used concentration for the synthesis of bPNIPAm with corresponding molecular weights of 2,500 and 5,000 g/mol are presented in **Table S3**. bPNIPAm was characterized by ¹H NMR (see **Figure S18** for bPNIPAm₅ ₖDₐ) and HABA titration assay (0.6 biotin for bPNIPAm₂.₅ ₖDₐ and 1.1 biotin for bPNIPAm₅ ₖDₐ).

Figures S16-S18 show the corresponding ¹H-NMR spectra of RAFT-PNIPAm-N₃-A, PNIPAM-N₃-A and bPNIPAm₅ ₖDₐ (**b13***) relating to the fabrication of PNIPAM chain with molecular weight of 5,000 g/mol. Analysis of ¹H NMR spectra gave that almost the desired ratio between initiator and monomer NIPAm has been established incorporating 22 monomers in RAFT-PNIPAm-N₃ for final bPNIPAm₂.₅ ₖDₐ (**b14***) and 40 monomers in RAFT-PNIPAm-N₃ for final bPNIPAm₅ ₖDₐ (**b13***).

5. Swelling-shrinking properties

Three different samples were studied: (i) Empty-Psome; (ii) in situ Avidin-Psome; (iii) post Avidin-Psome For each sample little amounts of 1 M HCl or 1 M NaOH were added to reach pH 5 or 8, respectively. This cycle was repeated 5 times and the hydrodynamic diameter was measured for both acidic and basic pH value by DLS. **Figure S2** shows the corresponding results.

6. Irradiation effect on the fluorescence of biotin-FITC-conjugated avidin

A 1 mg/mL of Avidin/bFITC solution was prepared in 1 mM PBS. Later, this sample was irradiated for 3, 6 or 9 min. Before and after irradiation samples were analyzed using fluorescence spectroscopy (λ_{exc} = 493 nm, λ_{obs} = 518 nm, C_{Avidin}= 0.1 mg/mL). All samples were studied at 0.25 mg BCP/mL. The experiments were carried out by triplicate (**Figure S1**).

7. Experimental description for preparing FITC-labeled Avidin-Psomes through the use of in situ and post loading method

Stock solutions: Avidin (1 mg/mL in 1 mM PBS, it was dissolved 1 day before and filtered with 0.1 µm), bFITC (2 mg/mL in DMSO/MilliQ). All the experiments were carried out in the darkness due to the presence of the dye. Formation of complex - The assembly is carried out using the following scheme: (a) start with filling the buffer, (b) add the amount of bFITC and (c) add the avidin solution. Let equilibrate 1 h in the cooler. Avidin/bFITC (3 mL of avidin 1 mg/mL in 1 mM PBS + 52 µL bPEGFITC solution (3Eq)).

For *in situ* loading method with avidin/bFITC the method of Gräfe et al. has been adopted and modified for avidin.[3] 16 mg of BCP1 were dissolved in 14.5 mL of 10 mM hydrochloric acid (pH 2), after complete dissolving this solution was passed through a 0.2 µm nylon filter. Then, in 13.5 mL the pH was adjusted around pH 5 by adding NaOH slowly, and it was added 1.5 mL of filtered solution of avidin/bFITC. Finally, to induce the self-assembly process, deprotonation of the tertiary amine moieties is performed by simply increasing the pH to a basic state (pH 8). After 3 days of stirring, the final polymersome structure is formed with a bilayer membrane. The final block copolymer concentration must be of 1 mg/mL and the avidin/bFITC concentration of 0.1 mg/mL. The polymersome solution was placed in the UV chamber and irradiated for 3 min in order to obtain robust and mechanically stable polymersomes. For *post* loading of Avidin/bFITC were studied 0.1 mg/mL of protein (12.5 mL of Psome 1 mg/mL + 300 µL of protein + 12.20 mL 2 mM PBS at pH 6). After mixing all samples were set to pH 6 and stirred overnight. The resulting solution was cleaned from non-enclosed protein using HFF or dialysis. The purification study and loading efficiency was carried using the same protocol than was described for in situ encapsulation.

The resulting solution in both loading methods was cleaned from non-enclosed protein using HFF or dialysis: (A) Using HFF (Membrane with MWCO 500 kDa): (i) HFF1 at pH 8, $V_{waste\ used}$ = 125 mL, 130 mbar; (ii) HFF2 at pH 7, $V_{waste\ used}$ = 100 mL, 130 mbar; (iii) HFF3 at pH 6, $V_{waste\ used}$ = 100 mL, 130 mbar. Before and after HFF purification samples (loading efficiency) and waste samples (purification monitoring) were analyzed using fluorescence spectroscopy (λ_{exc} = 493 nm, λ_{obs} = 518 nm). All samples were studied at 0.25 mg BCP/mL. The experiments were carried out by triplicate; (B) Using dialysis (Membrane with MWCO 1000 kDa), the sample was cleaned against 1 mM PBS pH 8, 7 and 6. Before and after dialysis purification samples (loading efficiency) and waste samples (purification monitoring,

0, 4, 8, 24 and 48 h) were analyzed using fluorescence spectroscopy (λ_{exc} = 493 nm, λ_{obs} = 518 nm). All samples were studied at 0.25 mg BCP/mL. The experiments were carried out by triplicate.

8. Calibration avidin AF4 + Fabrication of Avidin-Psomes through in situ and post loading method for AF4 study

For the calculation of avidin amounts, three different concentration series of pure avidin solutions were injected (100 µL of varied concentration) and separated by the specific separation profile. This calibration and quantification was carried out, but the results are not clear. Maybe there is an adsorption taking place on fresh membrane (**Figure S3**).

For the calculation of avidin amounts, three different concentration series of pure enzyme solutions were injected (100 µL of varied concentration) and separated by the specific separation profile. Recovery tests with varied sample loads verified that no adsorption takes place at fresh membranes. *Stock solutions:* BCP1 2 mg/mL in 0.01 M HCl; avidin 5 mg/mL in 1 mM PBS.

A. *Study on in situ loading method.* For in situ loading of avidin were studied 0.1 mg/mL of protein (2 mL of BCP1 + 1.92 mL 0.01M HCl + 80 µL protein). The final volume sample is 4 mL with a concentration of BCPs of 1 mg/mL. Then, the pH was changed to 8 and the solutions were stirred in the dark for 3 days. Afterwards the vesicles were crosslinked for 180 s and investigated by AF4. Study of *post* encapsulation.

B. *Study on post loading method.* For *post* encapsulation of avidin were studied 0.1 mg/mL of protein (1.25 mL of Psome 1 mg/mL + 25 µL of protein + 1225 µL 1 mM PBS at pH 6). The final volume in all samples is 2.5 mL with a concentration of Psomes of 0.5 mg/mL. After mixing all samples were set to pH 6 and stirred overnight. Afterwards the samples were investigated by AF4. Samples by AF4 and analyzed using 1 mM PBS at pH 8: Empty-Psome (0.5 mg of BCP/mL); in situ Avidin-Psomes (0.5 mg of BCP/mL + 0.05 mg/mL of avidin); *post* Avidin-Psomes (0.5 mg of BCP/mL + 0.05 mg/mL of avidin).

9. Additional study on the bioconjugate BC-HABA, consisting of Alexa Fluor-488-labeled avidin (AFF-488) and HABA, in absence and presence of biotin

a. Titration of free AFF-488 with HABA at pH 5

A solution of AFF-488 (1.52 µM) was prepared in 1 mM PBS at pH 5 and different equivalents of HABA ($C_{Stock\ HABA}$ = 1 mM) were added. The titration was monitored by fluorescence spectroscopy (**Figure S6-S8**).

b. Titration of BC-HABA with biotin

A solution of **BC-HABA** (3 µM of avidin AlexaFluor488) was prepared and different equivalents of biotin (375 µM) were added. The titration was monitored by fluorescence spectroscopy. With this experiment we can see that the fluorescence of the Alexa Fluor-488 dye is quenched by fluorescence

resonance energy transfer (FRET) to the quencher dye 2-(4′-hydroxyazobenzene) benzoic acid HABA (0 Eq Biotin). Later, when biotin is added, the HABA is displaced resulting in a corresponding increase in fluorescence. The only problem is that we could distinguish the number of biotins until 1.5 Eq, for more equivalents the fluorescence is the same. Two different excitation wavelengths and different pH were studied (**Figure S6**-**S8**).

c. Titration of AFF-488-loaded Psomes (AAP) with HABA at pH 6

To 2 mL of AAP solution (0.25 mg BCP/mL in 1 mM PBS pH 6) different concentrations of HABA were added (C_{HABA} = 1 mM at pH 6) (5, 10, 15, 20, 30, 40, 60, 80, 100, 120, 140, 160, 180, 200 µL) (Figure 4B main text).

d. HABA assay of biotinylated compound

To determine the apparent amount of coupled biotinylated compound (bcompound) to avidin the measured differences of absorbance values at Λ = 500 nm between [avidin/HABA] complex and [avidin/HABA]/bcompound mixtures and the linear regression of the lower part of the [avidin/HABA]/biotin titration curve were used to calculate the apparent amount of biotin moieties coupled to avidin (y = 0.0157 – 0.303x) (V_F = 500 µL, $C_{Avidin/HABA}$ = 6.25 µM) (30 Eq HABA). Assemble is carried out directly in the measurement cuvette using the following scheme: (a) start with filling the buffer, (b) add the amount of bcompound and (c) add the [avidin/HABA] complex solution. Let equilibrate overnight in the cooler. The resulting complex ([avidin/HABA]/bcompound) were measured in disposable UV microcuvettes by **UV/Vis** spectroscopy after 4 h of equilibration. The experiment was carried out by duplicate.

10. Fabrication of BC-HABA-loaded Psomes (HAAP) for carrying out FRET experiments and reference for FRET experiment (Figure 4)

Afterwards, the AFF-488 was in situ encapsulated in the polymersomes and crosslinked for 3 min followed by HFF purification (130 mbar, 150 mL, 1 mM PBS at pH 8) to remove the entire non-encapsulated AFF-488. The HFF step was monitored using the waste solution in order to optimize the optimal conditions (**Figure S22**). The encapsulation efficiency is 8.7 %, slightly higher than using Avidin/bFITC (Figure 1). During the purification process, some bFITC groups could be scattered by applied forces, partially reducing the fluorescence intensity recorded. It does not happen in the case of Alexa Fluor-488 dye due to its covalent bond.

The first trial was to form the avidin complex before encapsulation process, but for this complex a high excess of HABA is needed, and the most of the HABA is removed in the purification step (HFF) and it resulted in a not completed quenching effect. Therefore, the right procedure is to encapsulate just AFF-488 using in situ loading, crosslinking for 3 min, purify by HFF and, finally, add a right excess of HABA concentration. To adjust the right HABA concentration, a titration with HABA (0-25 µg/mL) in presence

of BC-HABA-loaded Psomes (0.25 mg BCP/mL) was carried out at pH 6 (Figure 3B). 25 µg/mL of HABA and 1 h incubation under stirring were chosen as optimal conditions.

In order to calculate the cumulative uptake (%), firstly next equation was used and then, to prepare the Figure 4 the obtained percentages are accumulated giving the % cumulative uptake.

$$\textbf{\% Docking ability} = (F(bx)-F(HAAP))/(F(AAP)-F(HAAP)) \times 100$$

F(bx): Fluorescence intensity obtained for each biotinylated biomolecule under different conditions

F(HAAP): Fluorescence intensity obtained for BC-HABA loaded Psomes (HAAP) - low signal

F(AAP): Fluorescence intensity obtained for AAF-488-loaded Psomes (AAP) - high signal- Reference 100% (see below the following figure)

In **Figure S22**, APP is A1-A3 and HAPP is A4-A6.
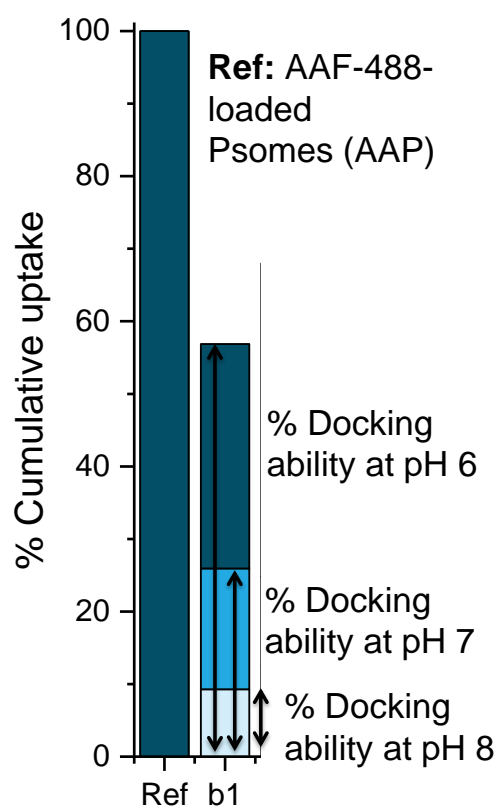
11. Additional Figures and Tables

Table S1. Used concentration for the synthesis of RAFT-PNIPAm-N3, including yield.

Polymer	RAFT-N$_3$	NIPAm	AIBN	Dioxane	Yield
	equivalent [mol] [mg]	equivalent [mol] [mg]	equivalent [mol] [mg]	[mL]	[g] [%]
RAFT-PNIPAm-N$_3$-A	1 2.23×10^{-4} 100	40 8.93×10^{-3} 1010	0.5 1.11×10^{-4} 18.3	3	1.04 94
RAFT-PNIPAm-N$_3$-B	1 4.47×10^{-4} 200	19 8.49×10^{-3} 962	0.5 2.23×10^{-4} 37	3	1.01 87

Table S2. Used concentration for the synthesis of PNIPAm-N$_3$, including yield

Polymer	RAFT-PNIPAm-N$_3$		TTMSS	AIBN	Dioxane	Yield
		equivalent [mol] [mg]	equivalent [mol] [mg]	equivalent [mol] [mg]	[mL]	[mg]
PNIPAm-N$_3$-A	RAFT-PNIPAm-N$_3$-A	1 1×10^{-4} 500	2 2×10^{-4} 50	0.5 5×10^{-5} 8.2	2	458
PNIPAm-N$_3$-B	RAFT-PNIPAm-N$_3$-B	1 2×10^{-4} 500	2 4×10^{-4} 100	0.5 1×10^{-4} 16.4	2	433

Table S3. Used concentration for the synthesis of bPNIPAm, including yield

Polymer		PNIPAm-N$_3$	bPEGCOD$_{500}$	H$_2$O/THF (1:3)	Yield
		equivalent [mol] [mg]	equivalent [mol] [mg]	[mL]	[mg]
bPNIPAm$_{5\ kDa}$	PNIPAm-N$_3$-A	1 2×10^{-5} 100	2 4×10^{-5} 22.0	10	102
bPNIPAm$_{2.5\ kDa}$	PNIPAm-N$_3$-B	1 2.4×10^{-5} 60	2 4.8×10^{-5} 26.4	6	65

Table S4. Specifications of block copolymer synthesized by ATRP

Composition	M$_w$ (g/mol)^a	M$_n$ (g/mol)^a	Đ (Mw/Mn)^a
PEG$_{45}$-b-(DEAEMA$_{78}$-s-DMIBM$_{23}$)	17200	18700	1.08

^{a}Molar mass distribution is determined by SEC. ^{b} Molecular weight is calculated by ^{1}H NMR

Table S5. List of the used biotinylated (bio)molecules used, their molecular weight and the used stock solutions for the corresponding experiments. All compounds were dissolved in 1 mM PBS. The same number of biotin groups were added in each compound.

Nomenclature Sample	Shape/Type of biomolecules	Molecular weight	Used stock solution (mg/mL)/(μM)	Biotin groups per molecule	Added volume (μL)
b1 bPEGNH$_2$ $_{500}$	Linear/neutral, PEG	410.95 g/mol	0.005/12	0.8	4.1
b2 bPEGNH$_2$ $_{3kDa}$	Linear/ neutral, PEG	3 kDa	0.025/8.5	0.8	5.9
b3 bPEGNH$_2$ $_{5kDa}$	Linear/ neutral, PEG	5 kDa	0.05/10	1.0	4.0
b4 bPEGNH$_2$ $_{10kDa}$	Linear/ neutral, PEG	10 kDa	0.1/10	0.8	5
b5 bTAT$_{2kDa}$	Linear/cationic, peptide	1918.5 g/mol	0.05/26	1.0	1.5
b6* bCPP$_{3kDa}$	Linear/ cationic, peptide	3011.9 g/mol	0.05/16.6	0.7	3.4
b7* bPPI$_{43kDa}$	Spherical/ cationic, glycodendrimer	43200 g/mol	0.5/11.5	1.2	2.9
b8 bHRP$_{44kDa}$	Spherical/cationic, enzyme	44 kDa	0.5/11.5	5.1	0.7
b9* bHA$_{7kDa}$	Linear/ anionic, nonsulfated glycosaminoglycan	7 kDa	0.1/14.5	1.0	2.8
b10* bHSA$_{66kDa}$	Spherical/ anionic, protein	66 kDa	1/15.0	1.0	2.6
b11 bGOx$_{160kDa}$	Spherical/ anionic, enzyme	Dimer/160 kDa	2.5/15.5	1.8	2.5
b12 bCAT$_{240kDa}$	Spherical/ anionic, enzyme	Tetramer/240 kDa	2.5/10.5	6.3	0.6
b13* bPNIPAm$_{5kDa}$	Linear/ neutral, polymer	5000 g/mol	0.05/10	1.1	3.6
b14* bPNIPAm$_{2.5kDa}$	Linear/ neutral, polymer	2500 g/mol	0.05/20	0.6	3.3

Table S6. Diameter of all used biotinylated compounds (C = 1 mg/mL in 1 mM PBS) studied by DLS and zeta potential.

Nomenclature	Sample	Shape/Type of biomolecules	Size (nm)	Zeta potential (mV)
b1	bPEGNH$_{2\ 500}$	Linear/neutral, PEG	≤1	-2.46
b2	bPEGNH$_{2\ 3kDa}$	Linear/ neutral, PEG	6,3	-1.25
b3	bPEGNH$_{2\ 5kDa}$	Linear/ neutral, PEG	3,8	-1.40
b4	bPEGNH$_{2\ 10kDa}$	Linear/ neutral, PEG	9,1	-0.57
b5	bTAT$_{2kDa}$	Linear/cationic, peptide	2,0	0.81
b6[*]	bCPP$_{3kDa}$	Linear/ cationic, peptide	> 500 nm	13.9
b7*	bPPI$_{43kDa}$	Spherical/ cationic, glycodendrimer	6,8	1.55
b8	bHRP$_{44kDa}$	Spherical/cationic, enzyme	6,7	-0.13
b9*	bHA$_{7kDa}$	Linear/ anionic, nonsulfated glycosaminoglycan	4,6	-1.5
b10*	bHSA$_{66kDa}$	Spherical/ anionic, protein	9,3	-6.23
b11	bGOx$_{160kDa}$	Spherical/ anionic, enzyme	13,1	-11.50
b12	bCAT$_{240kDa}$	Spherical/ anionic, enzyme	15,9	-9.25
b13*	bPNIPAm$_{5kDa}$	Linear/ neutral, polymer	3,9	-1.7
b14*	bPNIPAm$_{2.5kDa}$	Linear/ neutral, polymer	2,7	-16.6

Table S7. Hydrodynamic radius of the crosslinked polymersomes at pH 5 and pH 8.6 studied by DLS in MilliQ.

Time of crosslinking	pH 5	pH 8.6
90 s	77.2	51.7
3 min	65.7	52.3
5 min	62.3	52.5
10 min	60.1	52.7
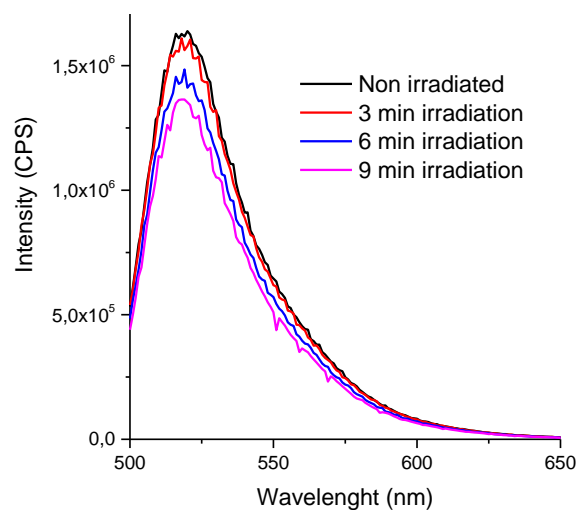
Figure S1. Effect of irradiation on Avidin/bFITC. Study of the fluorescence activity after 3 cycles of irradiation (λ_{exc} = 493 nm, λ_{obs} = 516 nm). Conditions: C_{Avidin} = 0.1 mg/mL
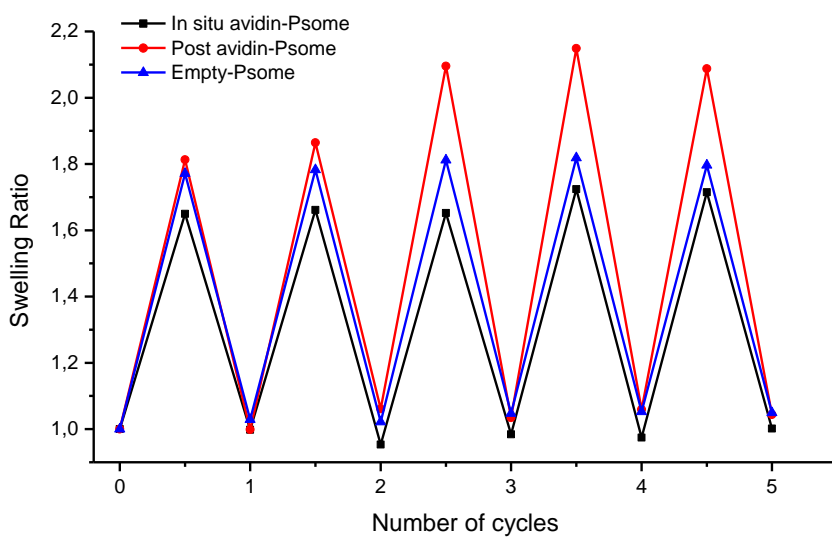
Figure S2. Swelling-shrinking properties of loaded and empty polymersome (Psome). C_{Psome} = 0.25 mg/mL in 1 mM PBS. Samples unpurified.
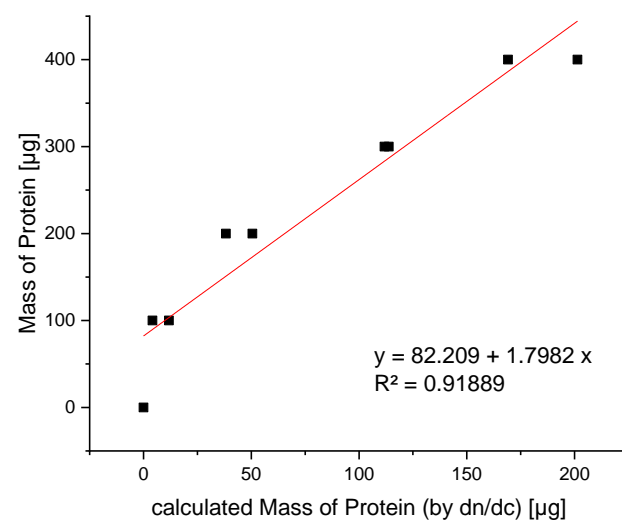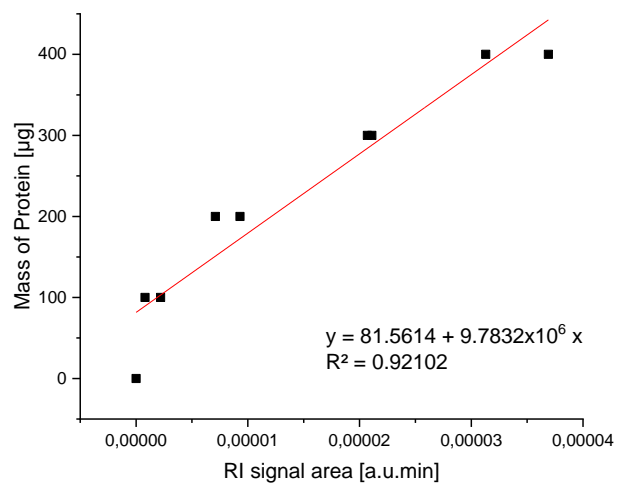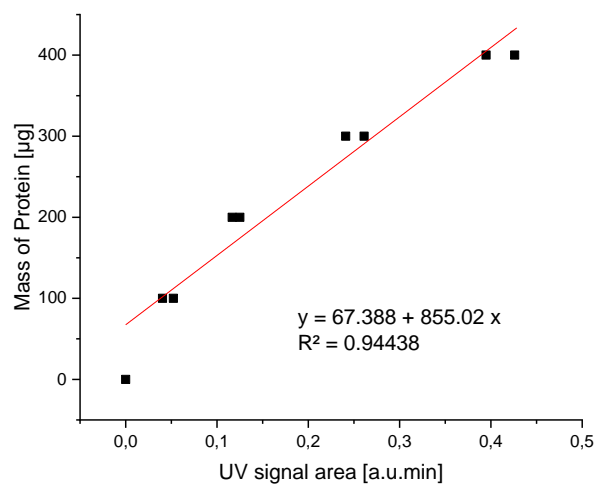
Figure S3. Calibration avidin using two different detectors (UV and RI), used for AF4 study.
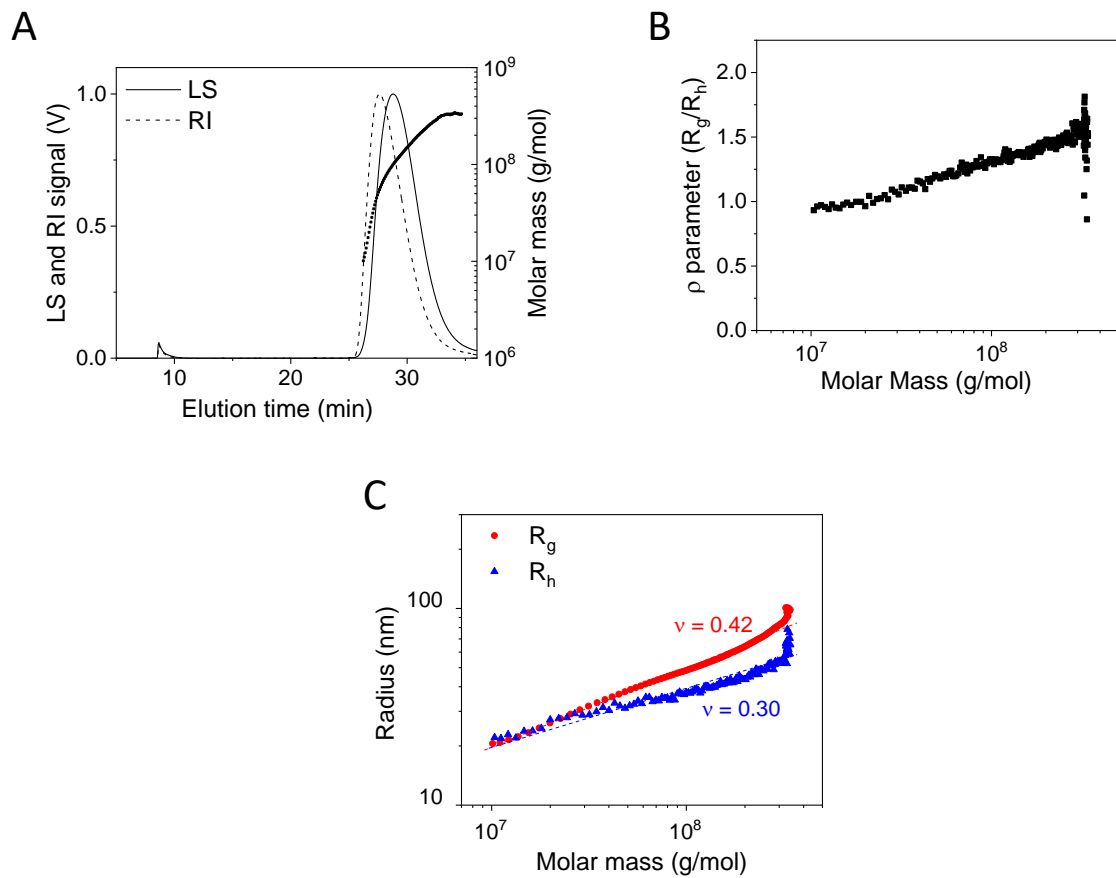
Measure-Ment	dn/dc (ml/g)	M_n (kg/mol)	M_w (kg/mol)	Đ (M_w/M_n)	N_{Assem}	R_g (nm)	R_h (nm)	ρ (R_g/R_h)
1. (300 µl)	0.183	54,900	102,000	1.86	2495	60.2	42.8	1.41
2. (300 µl)	0.183	58,700	104,000	1.77	2668	60.4	42.5	1.42
3. (300 µl)	0.183	54,700	102,000	1.86	2486	59.7	42.1	1.42
Average	0.183	56,100	102,000	1.82	2550	60.1	42.5	1.41

Figure S4. A) Fractogram of Avidin-Psome, molar masses, RI and LS signal vs. elution time. B) Rg/Rh vs molar mass. C) Scaling plots of R_g and R_h vs MM. *in situ* Avidin-Psome (C_{Psome} = 0.5 mg/mL + C_{Avidin} = 0.05 mg/mL)

A

B

C
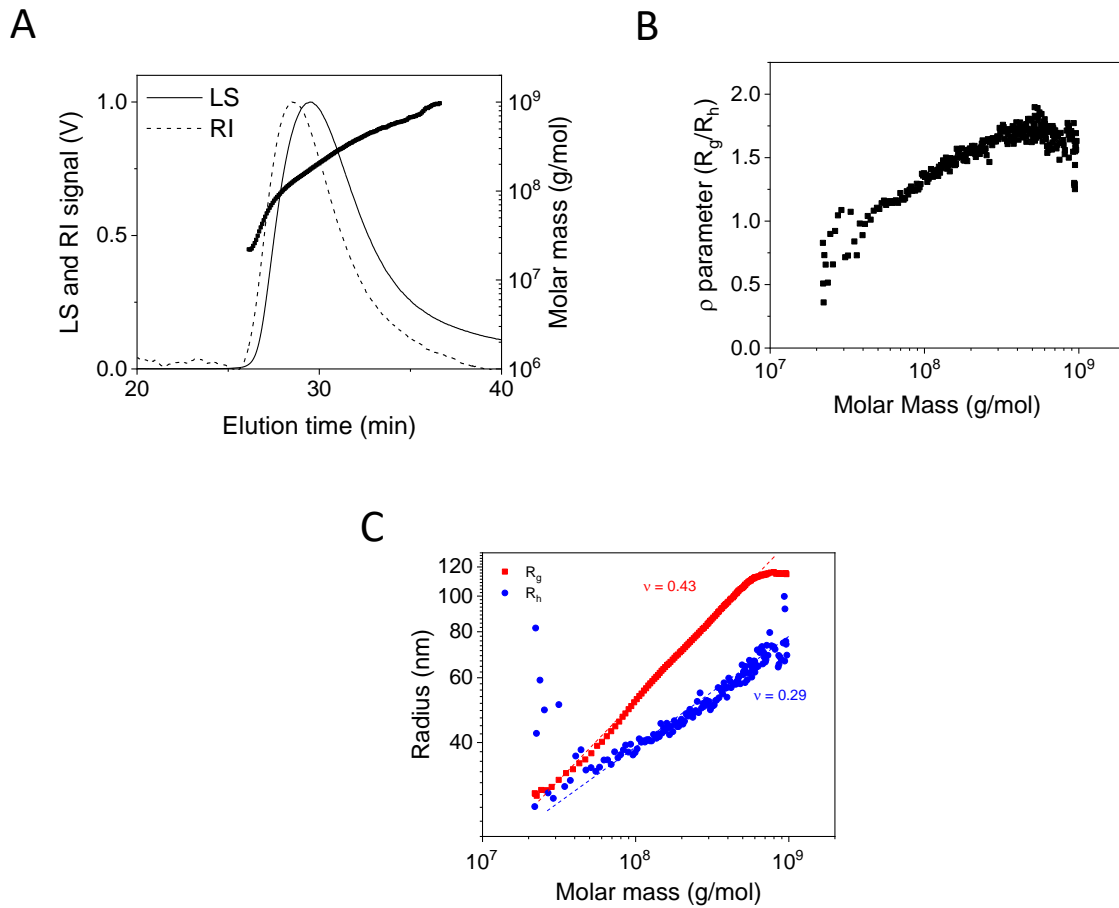
Measure-ment	dn/dc (ml/g)	M_n (kg/mol)	M_w (kg/mol)	Đ (M_w/M_n)	N_{Assem}	R_g (nm)	R_h (nm)	ρ (R_g/R_h)
1. (300 µl)	0.183	120,000	202,000	1.68	5455	82.9	53.0	1.56
2. (300 µl)	0.183	145,000	238,000	1.64	6591	89.1	54.2	1.64
3. (300 µl)	0.183	141,000	242,000	1.72	6409	92.6	54.8	1.69
Average	0.183	135,000	227,000	1.8	6136	88.2	54.0	1.63

Figure S5. A) Fractogram of Avidin-Psome, molar masses, RI and LS signal vs. elution time. B) R_g/R_h vs elution time. C) Scaling plot R_g vs MM. D) Scaling plot R_h vs MM. *post* Avidin-Psome (C_{Psome} = 0.5 mg/mL + C_{Avidin} = 0.05 mg/mL)
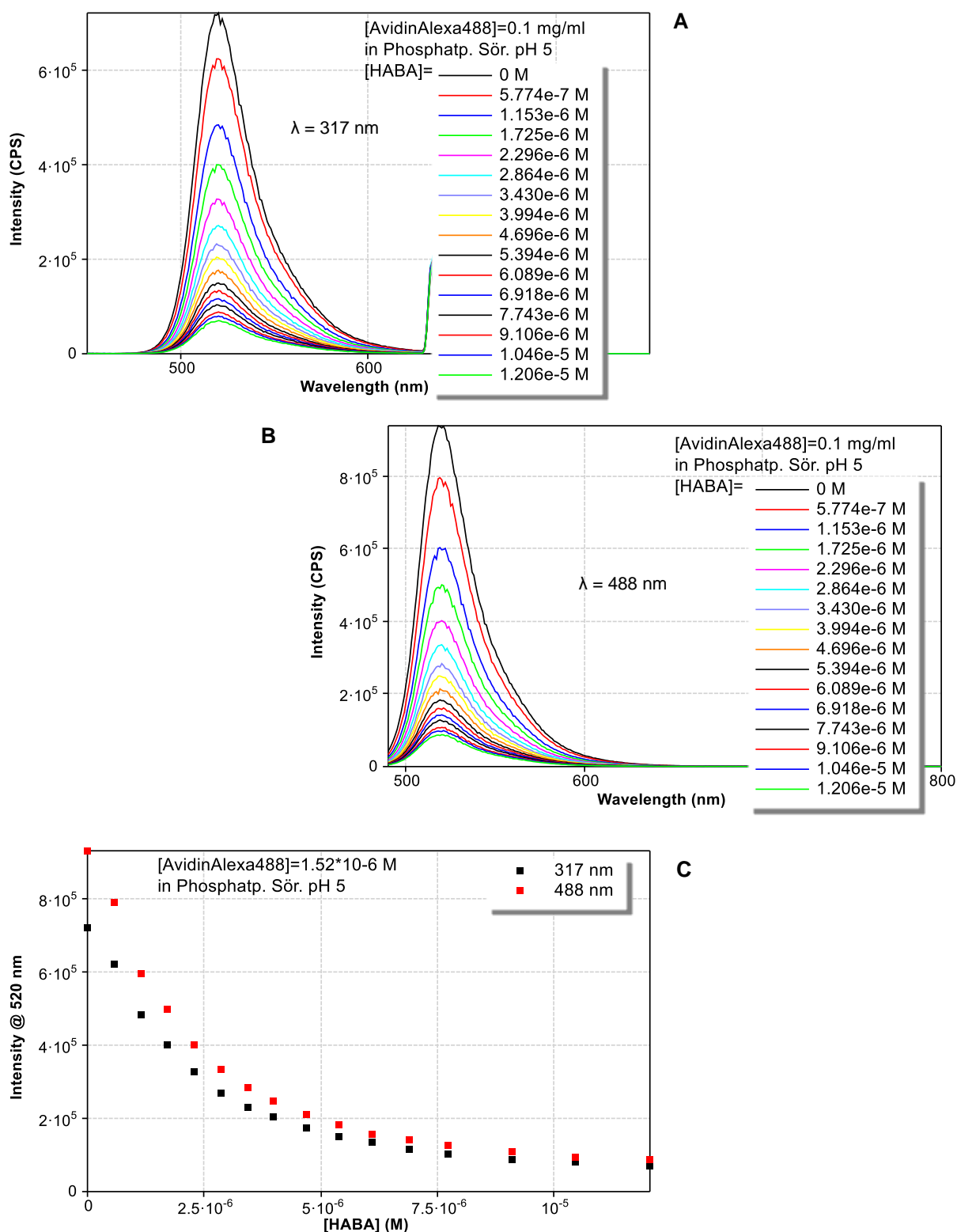
Figure S6. HABA titration of [AlexaFluor488/Avidin] by fluorescence intensity in 1 mM PBS pH 5. A) λ_{exc}: 317 nm; B) λ_{exc}: 488 nm; C) Comparison between both wavelengths using the maximum observed peak. [AlexaFluor488/Avidin/HABA] = 0.1 mg/mL. Reference: PBS pH 5.

A

B
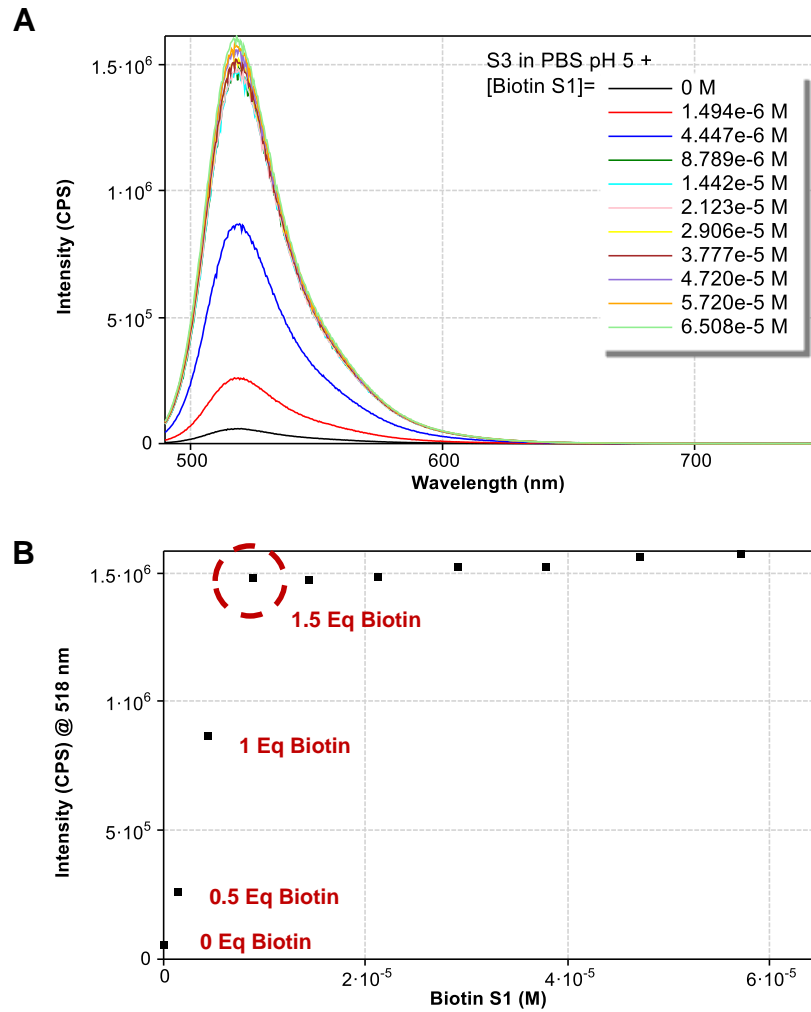
Figure S7. Biotin titration of [AlexaFluor488/Avidin/HABA] by fluorescence intensity in 1 mM PBS pH 5. Different concentrations of biotin were added. [AlexaFluor488/Avidin/HABA] = 3 µM Spectral band with:1 nm/1nm. Reference: PBS pH 5. Integration time: 0.2 s. λ_{exc}: 488 nm.

Results of **Figure S7** outline that only an increase of fluorescence for 1.5 eq biotin attached to Alexa Fluor 488-labeled avidin (AFF-488) is possible for one AFF-488 biomacromolecule. This also means that the attachment of more biotin ligands on AFF-488 is not detectable.
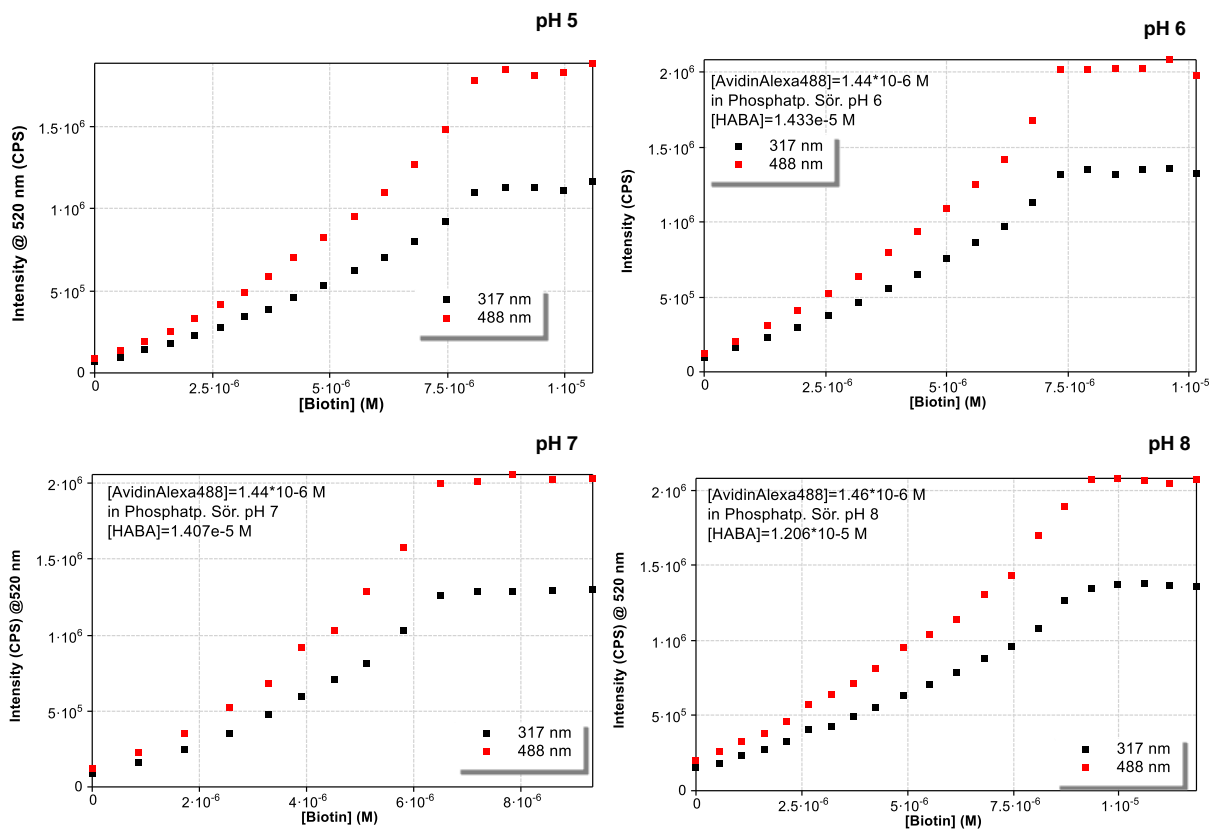
Figure S8. Biotin titration of [AlexaFluor488/Avidin/HABA] by fluorescence intensity in 1 mM PBS at pH 5, 6, 7 or 8. λ_{exc}: 317 nm and λ_{exc}: 488 nm. [AlexaFluor488/Avidin/HABA] = 1.45 μM.
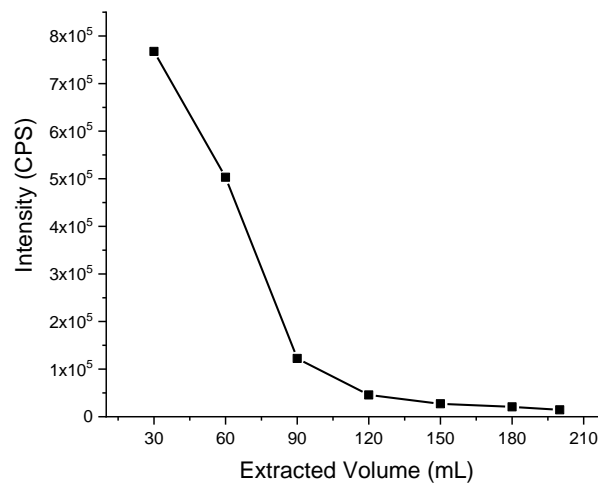
Figure S9. Monitoring of Avidin-Alexa488 Psome purification using HFF.
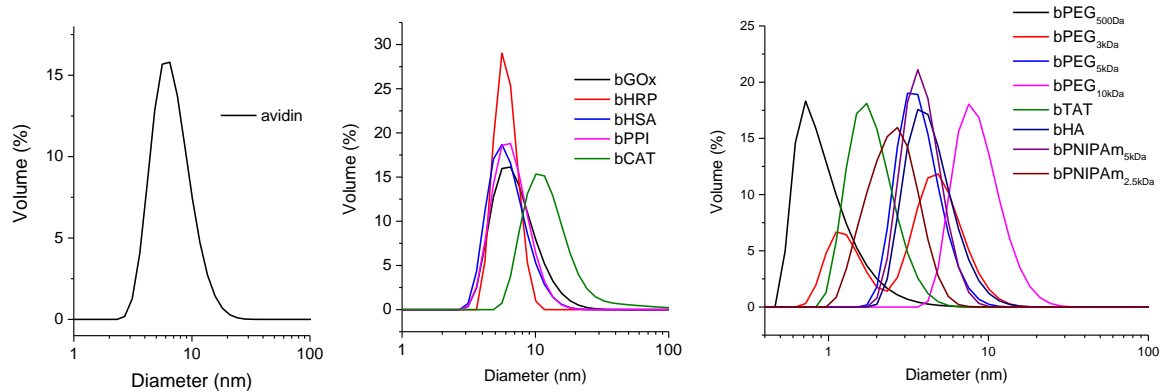
Figure S10. Diameter of avidin and all used biotinylated compounds (C = 1 mg/mL in 1 mM PBS) studied by DLS.
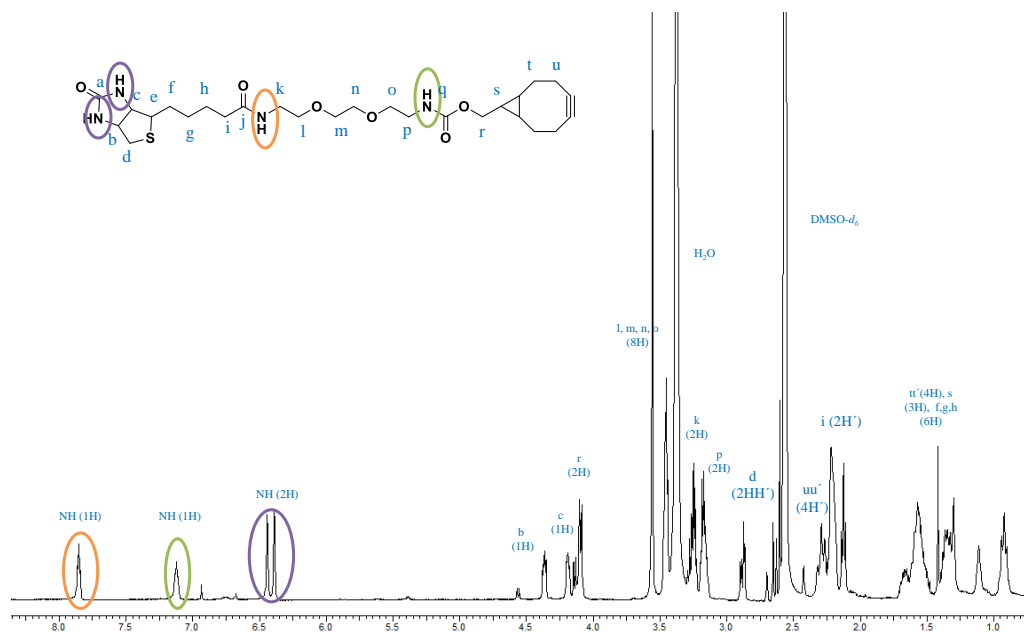
Figure S11. ¹H-NMR spectrum of biotinPEGCOD (500 Da) in DMSO-d_6.
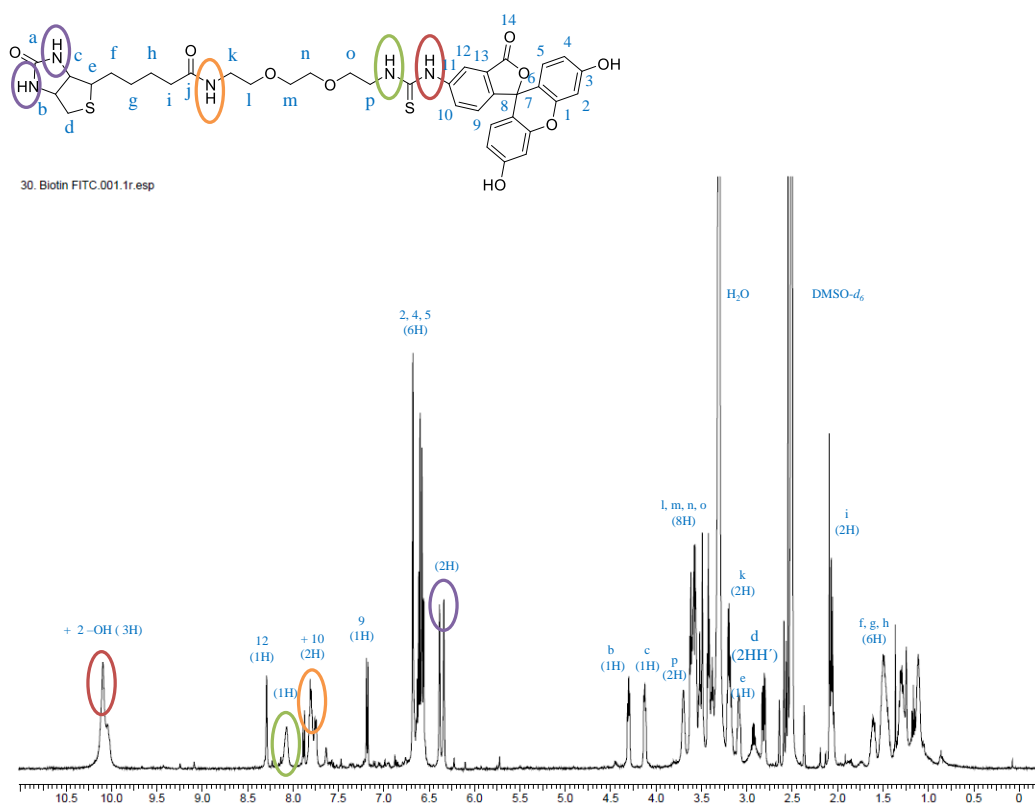
Figure S12. ^{1}H-NMR spectrum of biotinPEGFITC in DMSO-d_6.
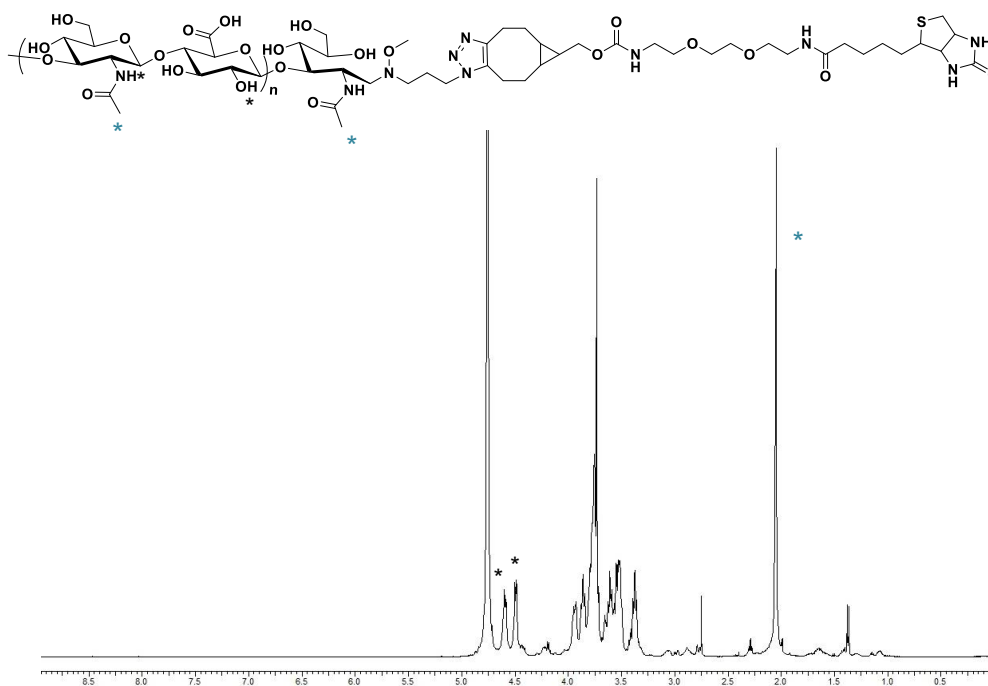
Figure S13. ^{1}H-NMR spectrum of **b9** (bHA) in D$_2$O.
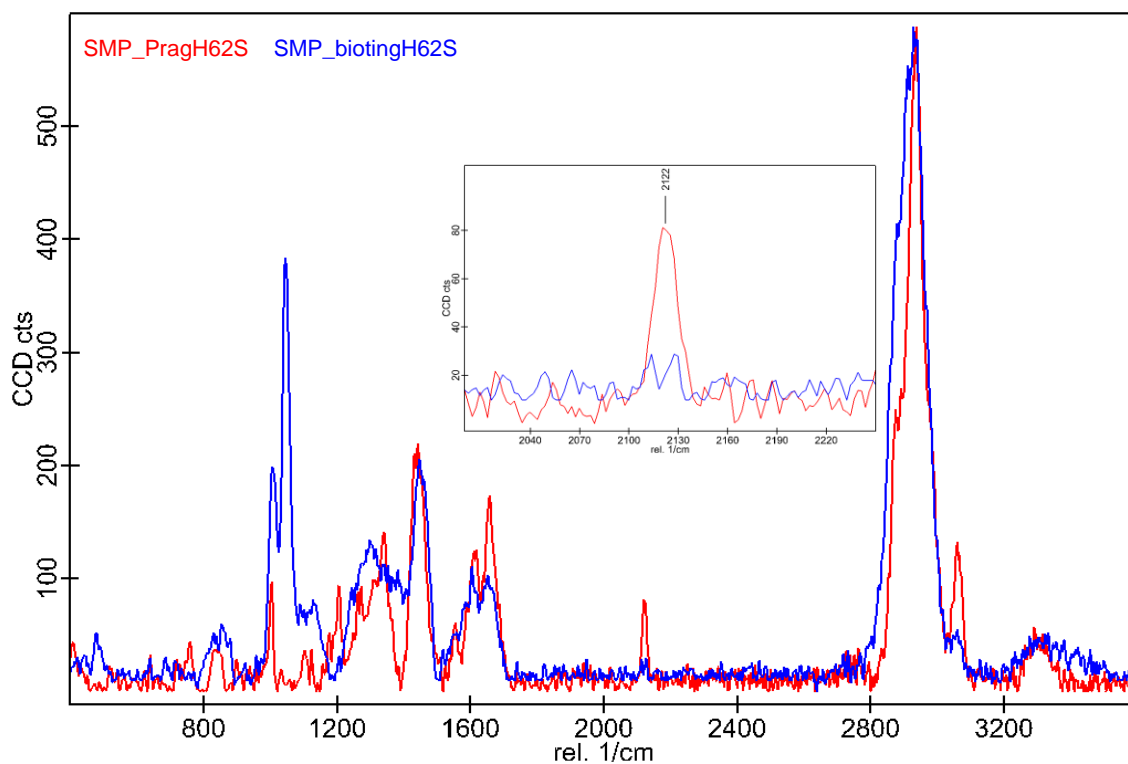
Figure S14. IR spectra of HA-N$_3$ (red line) and **b9 (**bHA) (blue line).
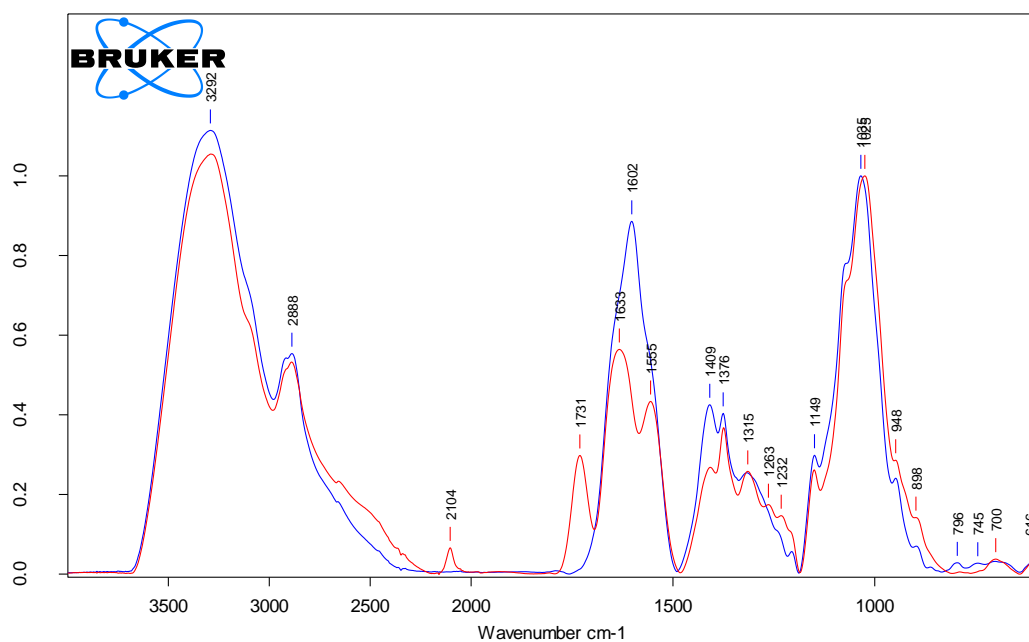
Figure S15. Raman spectra of CPP-Pra(red line) and **b6** (bCPP) (blue line).
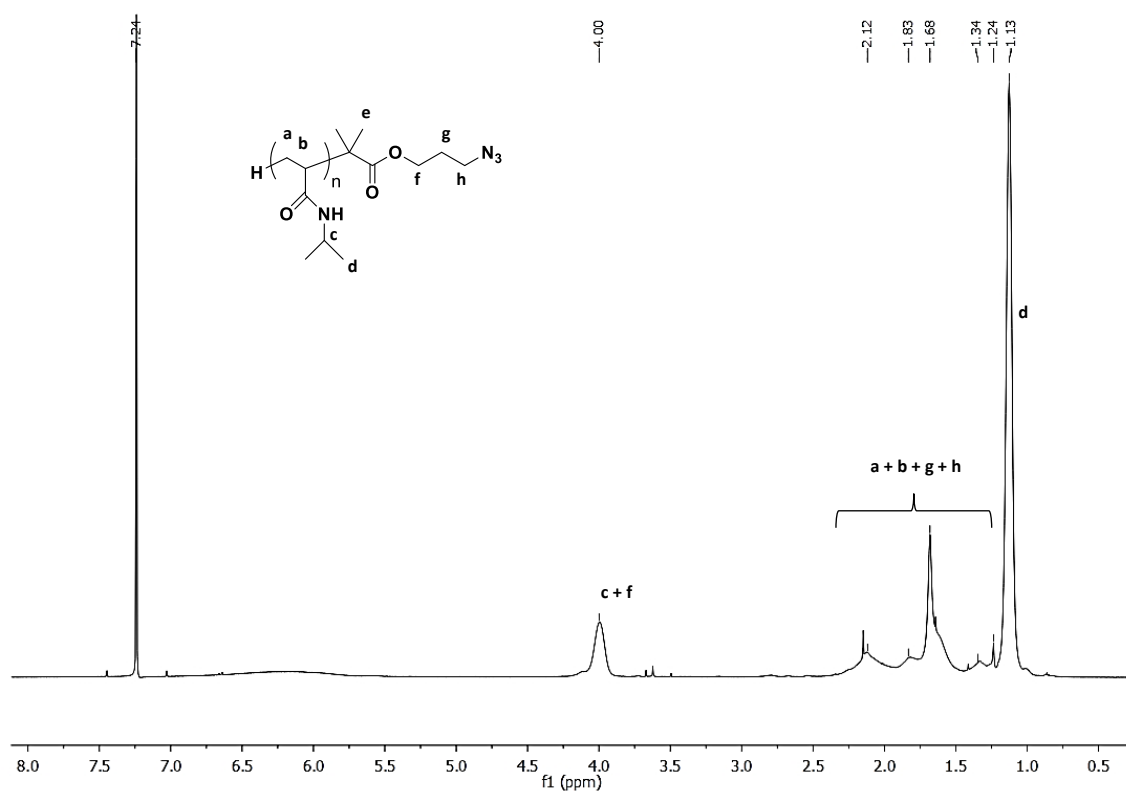
Figure S16. ^{1}H-NMR spectrum of protected PNIPAm (**8**) in CDCl$_3$.
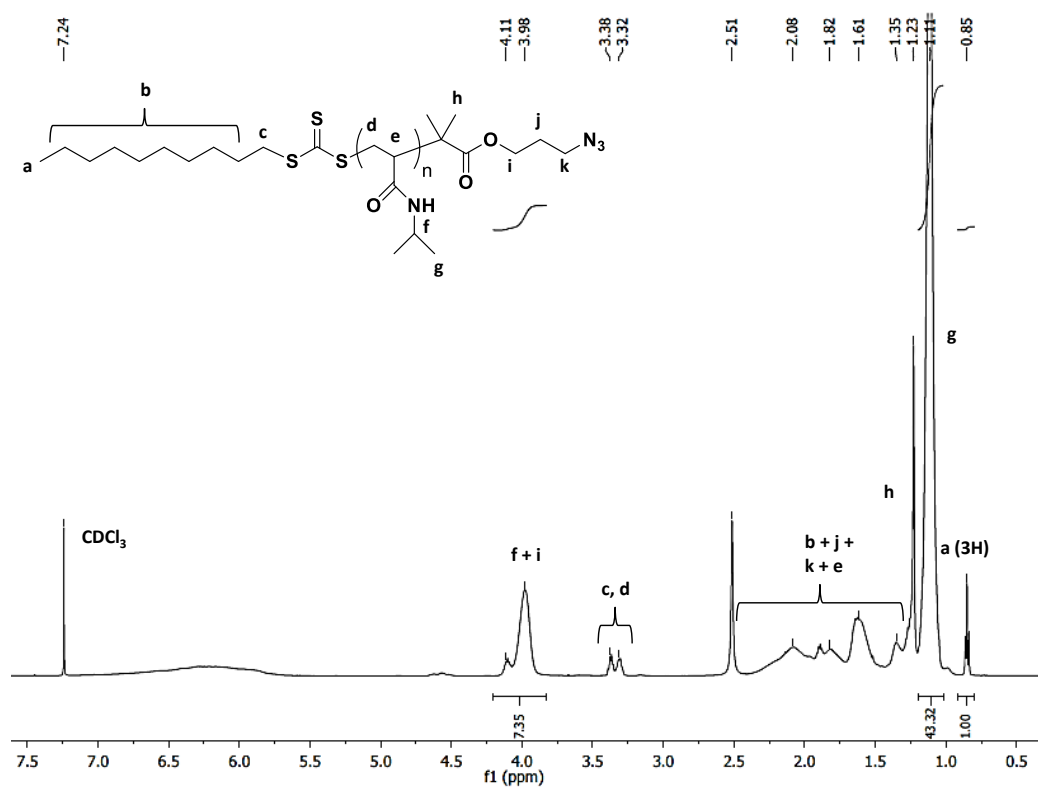
**Figure S17.** ^{1}H-NMR spectrum of unprotected PNIPAm (**10**) in CDCl$_3$.
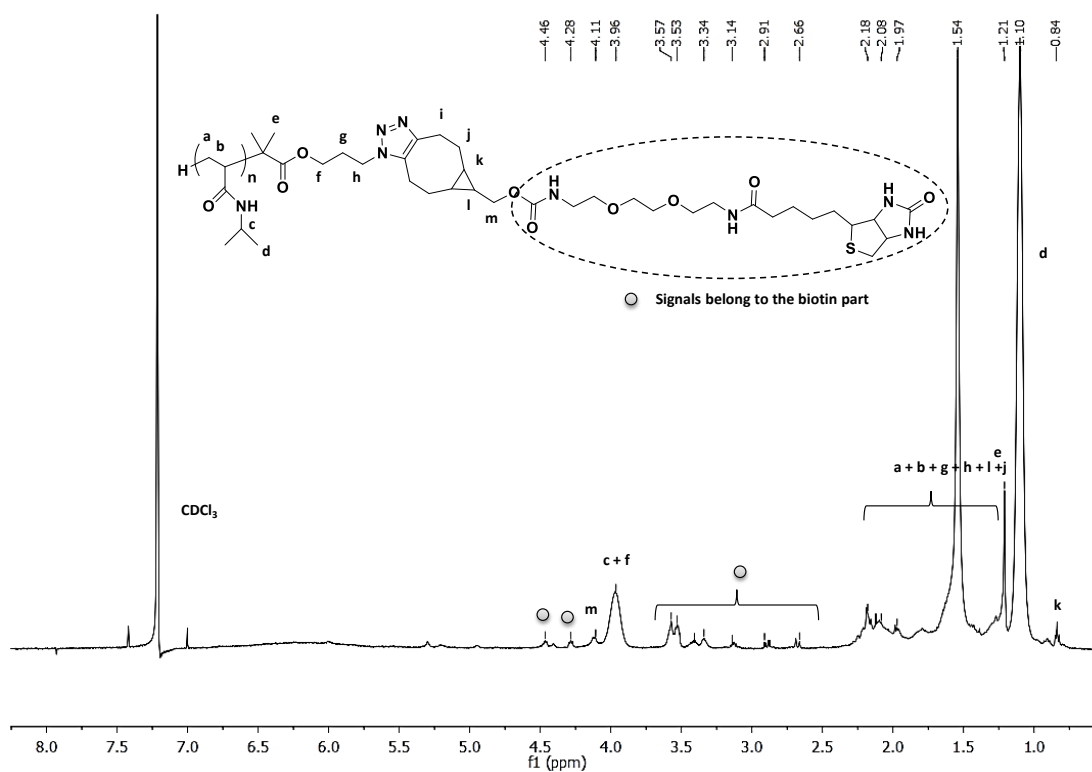
Figure S18. ^{1}H-NMR spectrum of bPNIPAm (**b14**) (**12**) in CDCl$_3$.
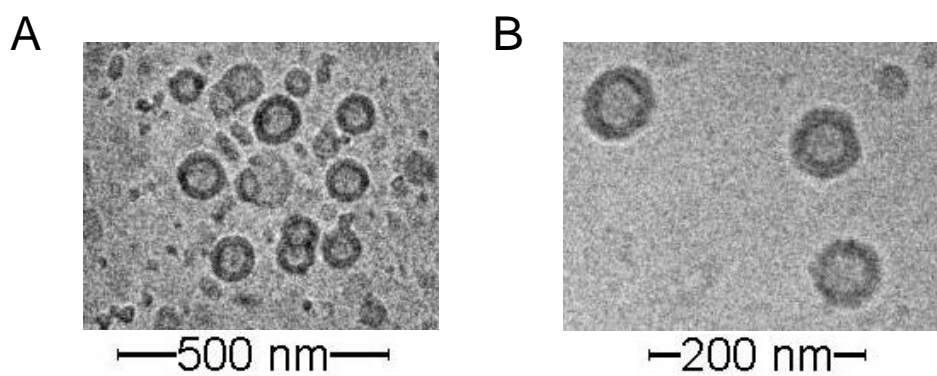
Figure S19. Cryo-TEM of the crosslinked polymersome (Empty-Psome) (C$_{Psome}$ = 1 mg BCP/mL, crosslinking time = 3 min) at pH 8. Diameter 74.5 $\pm$ 13 nm; Membrane thickness 16.0 $\pm$ 2.3 nm. Cryo-TEM of the avidin loaded crosslinked polymersome (In situ loading) (C$_{Psome}$ = 1 mg BCP/mL, 0.1 mg/mL avidin, crosslinking time = 3 min) at pH 8. Diameter 82.0 $\pm$ 19 nm; Membrane thickness 18.3 $\pm$ 3.9 nm.
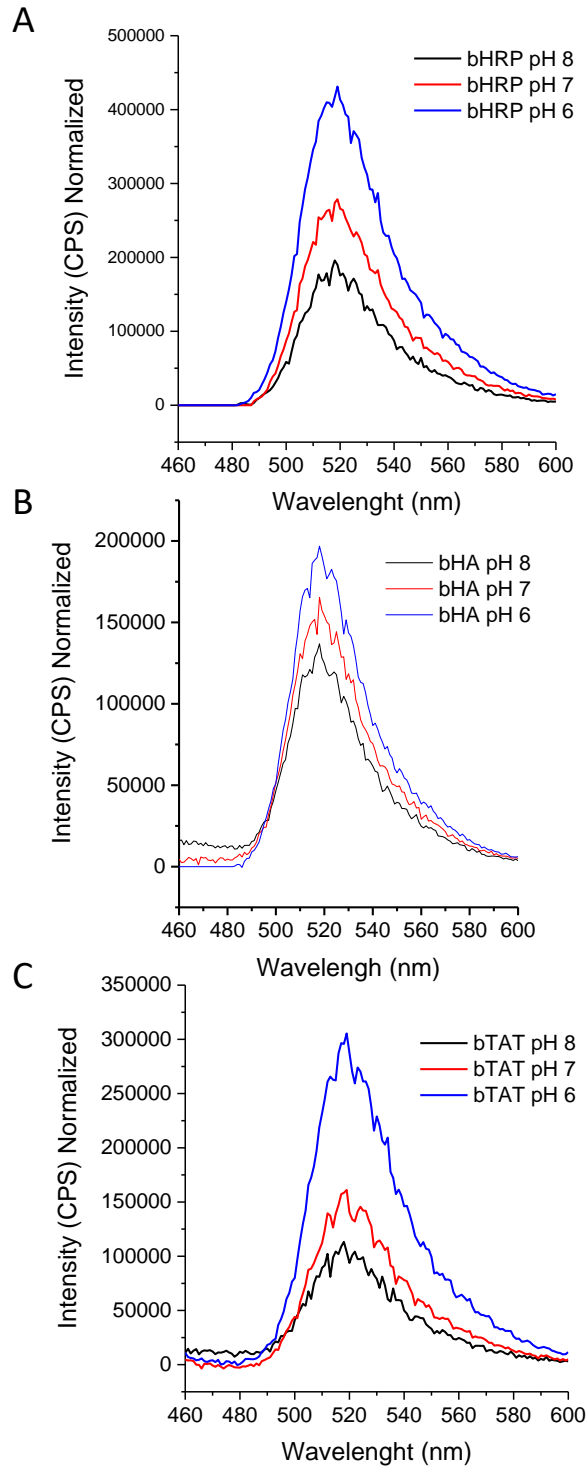
Figure S20. Individual permeability study of HAAP in presence of biotinylated compounds b8 (bHRP$_{44kDa}$) (A), b9 (bHA7$_{kDA}$) (B) and b5 (bTAT$_{2kDa}$) (C) at pH 8, 7 and 6. Results are not comparable between **Figure S20A**-**S20C** due to not using the same concentration on biotin ligand as done in the case for Figure 4.
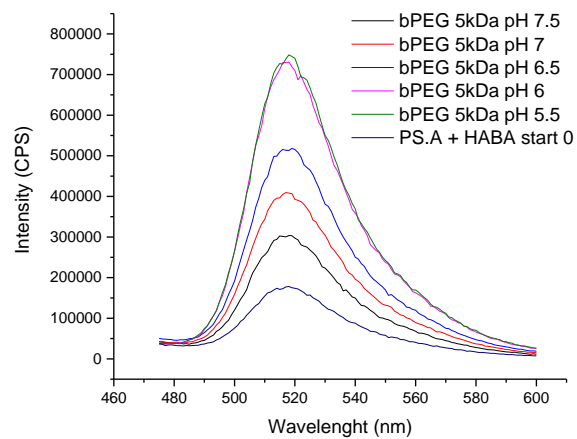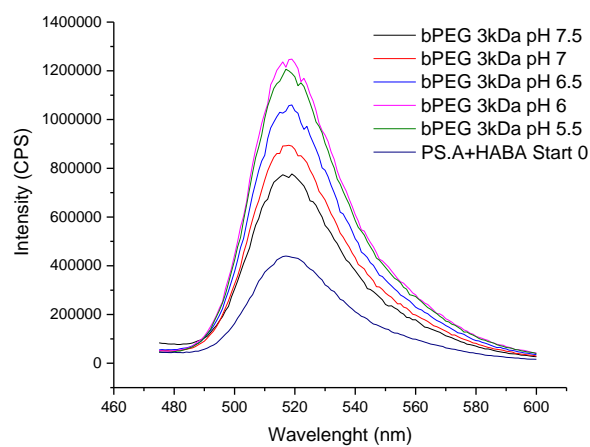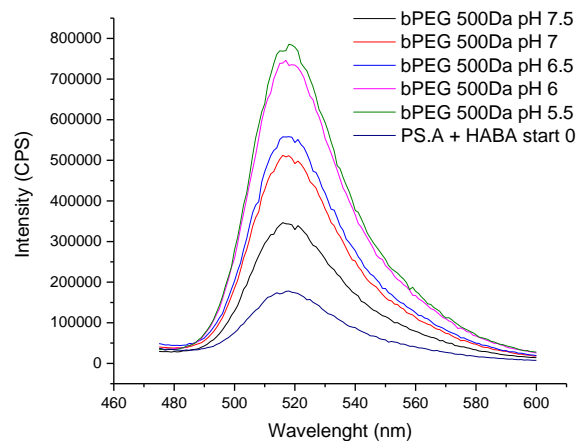
Figure S21. Individual permeability study of HAAP in presence of biotinylated compounds b1 (bPEG 500Da) (top), b2 (bPEG 3kDA) (middle) and b3 (bPEG 5kDa) (bottom) at pH 7.5, 7, 6.5, 6 and 5.5. Results are not comparable between top, middle and bottom due to not using the same concentration on biotin ligand as done in the case for Figure 4.
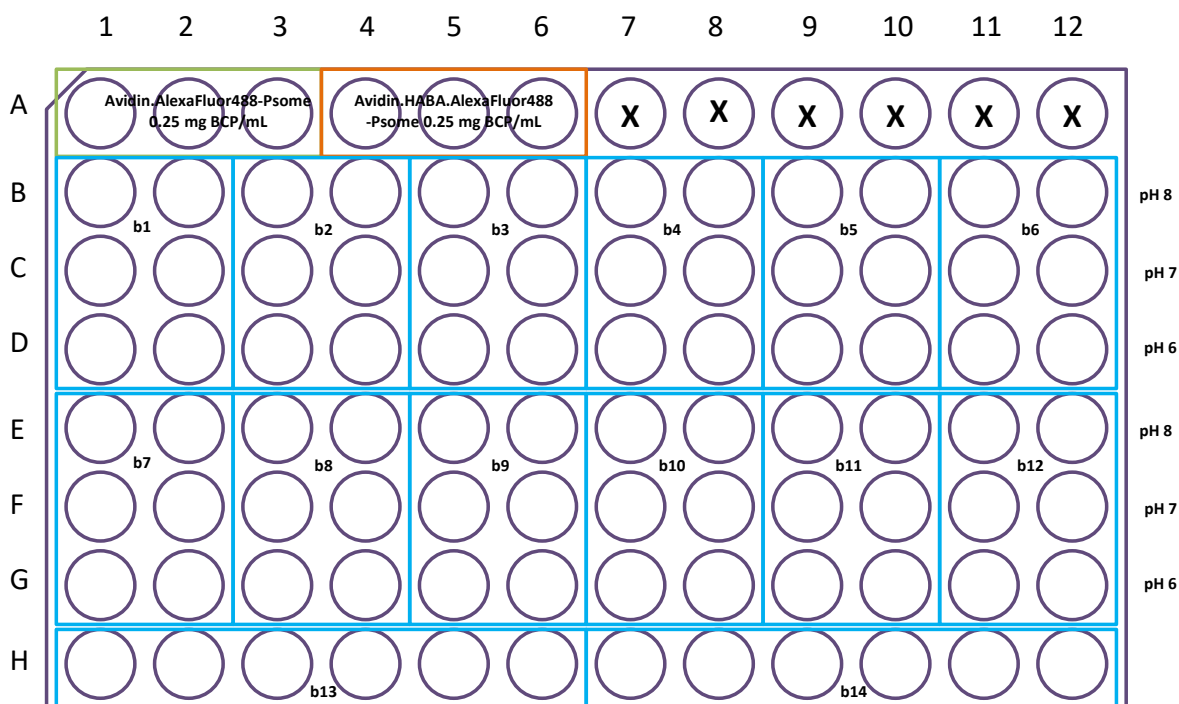
Figure S22. Template used in the microplate Reader for permeability study at different pH using biotinylated bio(macro)molecules.
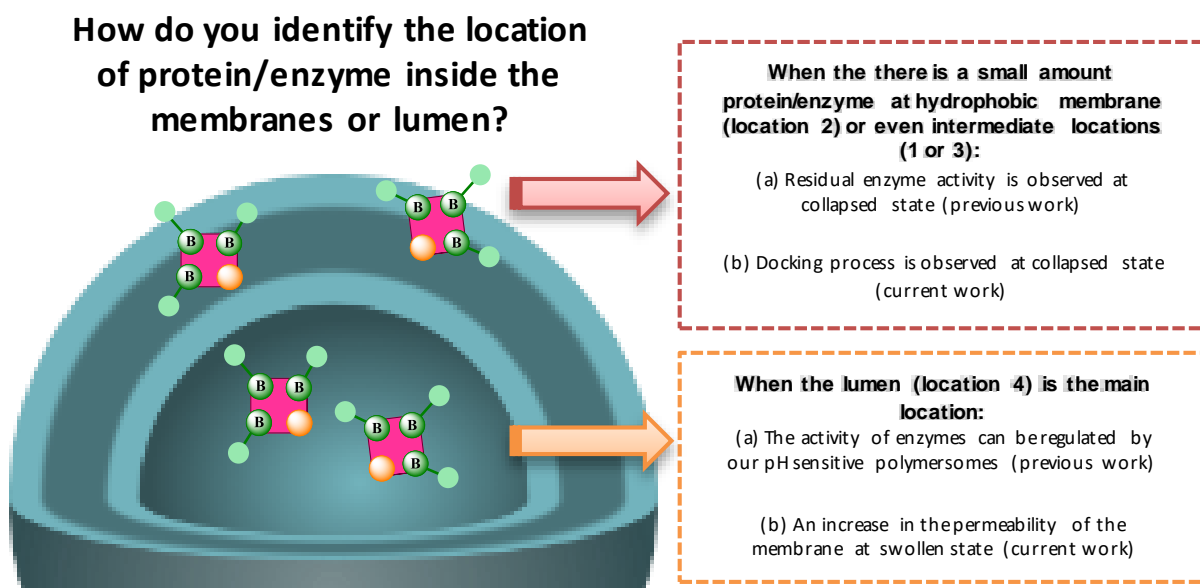
Figure S23. Representative outline of proposed locations throughout the manuscript.

12. References

1. Burchard, W. "Solution Properties of Branched Macromolecules" in *Branched Polymers II*, Springer, 1999, pp. 113-194.

2. Ccorahua, R.; Moreno, S.; Gumz, H.; Sahre, K.; Voit, B.; Appelhans, D. Reconstitution properties of Biologically Active Polymersomes after Cryogenic Freezing and Freeze-Drying Process. *RSC Adv*. **2018**, *8* (45), 25436-25443.

3. Gaitzsch, J.; Appelhans, D.; Grafe, D.; Schwille, P.; Voit, B. Photo-crosslinked and pH Sensitive Polymersomes for Triggering the Loading and Release of Cargo. *Chem.Commun.* **2011**, *47* (12), 3466-3468.

4. Gräfe, D.; Gaitzsch, J.; Appelhans, D.; Voit, B. Crosslinked Polymersomes as Nanoreactors for Controlled and Stabilized Single and Cascade Enzymatic Reactions. *Nanoscale* **2014**, *6* (18), 10752-10761.

5. Gumz, H.; Lai, T. H.; Voit, B.; Appelhans, D. Fine-tuning the pH Response of Polymersomes for Mimicking and Controlling Cell Membrane Functionality. *Polym. Chem*. **2017**, *8* (19), 2904-2908.

6. Tarallo, R.; Accardo, A.; Falanga, A.; Guarnieri, D.; Vitiello, G.; Netti, P.; D'Errico, G.; Morelli, G.; Galdiero, S. Clickable Functionalization of Liposomes with the gH625 Peptide from *Herpes simplex* Virus Type I for Intracellular Drug Delivery. *Chemistry* **2011**, *17* (45), 12659-12668.

7. Ennen, F.; Boye, S.; Lederer, A.; Cernescu, M.; Komber, H.; Brutschy, B.; Voit, B.; Appelhans, D. Biohybrid Structures Consisting of Biotinylated Glycodendrimers and Proteins: Influence of the Biotin Ligand´s Number and Chemical Nature on the Biotin-Avidin Conjugation. *Polym. Chem*. **2014**, *5* (4), 1323-1339.

8. Upadhyay, K. K.; Le Meins, J. F.; Misra, A.; Voisin, P.; Bouchaud, V.; Ibarboure, E.; Schatz, C.; Lecommandoux, S. Biomimetic Doxorubicin Loaded Polymersomes from Hyaluronan-block-Poly(ɣ-benzyl-glutamate) copolymers. *Biomacromolecules* **2009**, *10* (10), 2802-2808.